The Canadian Mineralogist
Vol. 42, pp. 63-86 (2004)

THE SYSTEM Fe–Co–Ni–As–S. II. PHASE RELATIONS IN THE (Fe,Co,Ni)$As_{1.5}S_{0.5}$ SECTION AT 650° AND 500°C

SKAGE R. HEM[§] AND EMIL MAKOVICKY

Geological Institute, University of Copenhagen, Østervoldgade 10, DK–1350 København K, Denmark

ABSTRACT

The diarsenides and sulfarsenides of Fe, Co and Ni have a widespread geological occurrence; they exhibit complex paragenetic and compositional relations, and are commonly associated with economically important minerals, such as PGM and gold. These minerals have been investigated at 500° and 650°C, with a focus on phase relations within the arsenic-rich regions of the $(Fe,Co,Ni)(As,S)_2$ prism. The phase relations involve alloclasite, arsenopyrite, cobaltite or gersdorffite, in equilibrium with diarsenide solid-solution (*dss*), löllingite, krutovite or safflorite. Coexisting skutterudite and pyrrhotite occur in equilibria with all the above-mentioned phases except krutovite. At 650°C, most of the phases exhibit extensive substitution, both with regard to Fe–Co–Ni and As–S. There are complete solid-solutions between safflorite (*dss*), alloclasite, skutterudite, and their respective ($Fe_{0.5}Ni_{0.5}$) analogues. There is also a complete solid-solution between cobaltite and gersdorffite. At 500°C, these solid-solutions are more restricted with respect to Fe–Co–Ni, but they still show a large variation in As–S contents. The observed assemblages and solid-solution limits agree well with their natural counterparts, although skutterudite and pyrrhotite very rarely occur together in nature.

Keywords: alloclasite, arsenopyrite, cobaltite, gersdorffite, diarsenides, krutovite, löllingite, rammelsbergite, safflorite, skutterudite, sulfarsenides, phase relations.

SOMMAIRE

On trouve les diarséniures et les sulfarséniures de Fe, Co et Ni dans plusieurs contextes géologiques. Ils font preuve de relations paragénétiques et compositionnelles complexes, et sont à plusieurs endroits associés à des minéraux économiquement importants, par exemple les minéraux du groupe du platine et l'or. Nous avons étudié ces phases à 500° et à 650°C, en nous attardant aux relations de phases dans les régions riches en arsenic du prisme $(Fe,Co,Ni)(As,S)_2$. Ces relations de phases impliquent alloclasite, arsénopyrite, cobaltite ou gersdorffite, en équilibre avec une solution solide de diarséniures (*dss*), löllingite, krutovite ou safflorite. La skutterudite et la pyrrhotite sont en équilibre avec toutes ces phases sauf la krutovite. A 650°C, la plupart des phases citées font preuve de solution solide importante, tant par rapport à Fe–Co–Ni qu'à As–S. Il y a solution solide complète entre safflorite (*dss*), alloclasite, skutterudite, et leurs analogues ($Fe_{0.5}Ni_{0.5}$) respectifs. Il y a aussi une solution solide complète entre cobaltite et gersdorffite. A 500°C, ces solutions solides sont plus restreintes par rapport à Fe–Co–Ni, mais la variation est toujours aussi grande qu'à 650°C dans les teneurs As–S. Les assemblages observés et les limites de solubilité concordent bien avec les équivalents naturels, quoique skutterudite et pyrrhotite ne sont que très rarement associées dans la nature.

(Traduit par la Rédaction)

Mots-clés: alloclasite, arsénopyrite, cobaltite, gersdorffite, diarséniures, krutovite, löllingite, rammelsbergite, safflorite, skutterudite, sulfarséniures, relations de phases.

INTRODUCTION

Minerals were synthesized in the system Fe – Co – Ni – As – S with the purpose of establishing the phase relations between sulfarsenides and diarsenides. The bulk composition of the charges was made equal to $(Fe,Co,Ni)As_{1.5}S_{0.5}$, and these minerals were synthesized at 650° or 500°C. Parallel investigations of the phase equilibria between sulfarsenides and disulfides, *i.e.*, bulk compositions equal to $(Fe,Co,Ni)As_{0.5}S_{1.5}$, are reported in the companion paper (Hem & Makovicky 2004). The experimental products were investigated by electron microprobe and X-ray powder diffraction. In this paper, we report equilibria involving alloclasite, arsenopyrite, cobaltite, gersdorffite, diarsenide solid-solution, krutovite, löllingite, pyrrhotite, safflorite and skutterudite.

§ *E-mail address*: skage@geol.ku.dk

Review of the Minerals of Relevance to this Study

In Table 1, we list the minerals of direct relevance to this study.

The solid-solution series of cubic triarsenides can be described by the general formula $(Fe,Co,Ni)As_{3-x}$, and includes the minerals skutterudite ($CoAs_{3-x}$) and nickel-skutterudite [$MeAs_{3-x}$, *Me* = Fe, Co, Ni and (Fe,Co) < Ni]. This solid-solution series extends from the pure Co end-member to Co-free compositions, in which Co is replaced by a mixture of Fe and Ni (Roseboom 1962, Nickel 1970). Substantial amounts of Sb and Bi can substitute for As (Laroussi 1990), and the arsenic to metal ratio is commonly reported to be lower than the ideal value of three. Nickeline (NiAs) and pyrrhotite ($Fe_{1-x}S$) are hexagonal or pseudohexagonal phases with related structures, both with anions in trigonal prismatic coordination and octahedrally coordinated metals. The crystallography and phase relations of pyrrhotite are complex, and interested readers are referred to Craig & Scott (1974), Kotny *et al.* (2000) and Pósfai *et al.* (2000). The sulfarsenides of Fe, Co and Ni are: arsenopyrite (FeAsS), alloclasite ($CoAs_{1+x}S_{1-x}$), cobaltite (CoAsS) and gersdorffite (NiAsS). The Co-dominant analogue of arsenopyrite has also been referred to as glaucodot, but for the purpose of this study, all members of the solid-solution series are called arsenopyrite. All these sulfarsenides have a structure in which the metal atom is in octahedral coordination. The anions are tetrahedrally coordinated to three metal atoms and one anion. The cobaltite and gersdorffite structures are derived from that of pyrite. Every metal octahedron shares each corner with two other metal octahedra, thereby forming groups of three. Such groups form a three-dimensional network stabilized by anion–anion bonds that link together the central anions of adjacent groups. The arsenopyrite and alloclasite structures are derivatives of the marcasite structure, in which the metal octahedra share edges along *c* and corners in the *a*–*b* plane. The same general principle is followed by löllingite ($FeAs_2$) rammelsbergite ($NiAs_2$) and safflorite ($CoAs_2$). In all these phases Fe, Co and Ni substitute for each other, as do As and S.

Several studies of the phase relations in this system have been undertaken (Table 2). The authors cited investigated two- to four-component subsystems of the system Fe–Co–Ni–As–S. The purpose of the work of Klemm (1965a) was somewhat similar to ours, in that he investigated the temperature dependence of the (Fe,Co,Ni)AsS solid-solutions and suggested their application as a geothermometer. His results have been applied to several natural deposits (*e.g.*, Misra & Fleet 1975, Oen *et al.* 1984, Gervilla *et al.* 1996, Hem *et al.* 2001), in some cases yielding results that contradict other indicators of temperature. Misra & Fleet (1975) suggested that the discrepancy was caused by the As ⇔ S substitution, which was not dealt with by Klemm (1965a). Indeed, extensive solid-solution involving As and S adds a degree of variance to the system, making the solvus diagram of Klemm (1965a) of limited use for geothermometry. Such substitution is

TABLE 1. PHASES OF RELEVANCE TO THIS STUDY OF THE SYSTEM Fe–Co–Ni–As–S

Phase	Ideal composition	Structure type
Nickeline	NiAs	Octahedrally coordinated metals bound to anions in trigonal prismatic coordination
Pyrrhotite	$Fe_{1-x}S$	NiAs type with different distributions of Fe vacancies
Langisite	CoAs	NiAs
Jaipurite	CoS	NiAs
Alloclasite	CoAsS	Marcasite type with ordered As–S groups
Arsenopyrite	FeAsS	Marcasite type, monoclinic or triclinic
Diarsenide solid-solution	$MeAs_2$	Marcasite type with short *c*-axis
Löllingite	$FeAs_2$	Marcasite type with short *c*-axis
Rammelsbergite	$NiAs_2$	Marcasite type
Safflorite	$CoAs_2$	Marcasite type, orthorhombic or monoclinic
Pararammelsbergite	$NiAs_2$	Structure is transitional between pyrite and marcasite
Cobaltite	CoAsS	Pyrite type, cubic or orthorhombic due to As–S ordering
Gersdorffite	NiAsS	Pyrite type, cubic or orthorhombic due to As–S ordering
Krutovite	$NiAs_2$	Pyrite type
Skutterudite	$CoAs_3$	Octahedrally coordinated metals bound to As_4 groups

In all the above-mentioned phases, Fe, Co and Ni substitute for each other, as do As and S. In the NiAs-type structures, the extent of As-for-S substitution is very limited.

TABLE 2. PREVIOUS INVESTIGATIONS IN THE SYSTEM Fe–Co–Ni–As–S

Author	System	T	Notes
Barton (1969)	Fe–As–S	281–825°C	Compositions indirectly derived from PXRD
Clark (1960)	Fe–As–S	400–750°C	Compositions found by wet-chemical method
Roseboom (1962)	Fe–Co–Ni$(As)_3$	600–800°C	The temperature dependence of the solid-solution is not fully described
Roseboom (1963)	Fe–Co–Ni$(As)_2$	800°C	The emphasis in this work is on diarsenides only
Yund (1962)	Ni–As–S	700, 450°C	Compositions indirectly derived from PXRD
Klemm (1965a)	Fe–Co–Ni(AsS)	300–650°C	Only two phases found; the As:S ratio was not investigated
Maurel & Picot (1974)	Co–Ni–$(As,S)_2$	700–1000°C	Very high temperature compared to natural assemblages
Kretschmar & Scott (1976)	Fe–As–S	281–825°C	Focused on the arsenopyrite geothermometer

well documented in both synthetic and natural assemblages (Yund 1962, Petruk *et al.* 1971, Maurel & Picot 1974, Misra & Fleet 1975, Kretschmar & Scott 1976).

The phase equilibria determined in the present study are pertinent to complex Co–Ni–As–Ag deposits, such as those of the Cobalt District, Ontario (Petruk *et al.* 1971) and Bou Azzer, Morocco (En Nacri 1995). In some of these deposits, the temperatures investigated represent the absolute peak temperature of formation, determined by the rammelsbergite – pararammelsbergite transformation, which occurs at 590°C or lower (Yund 1962), although most of the occurrences of this type form at substantially lower temperatures.

In magmatic ore assemblages, the temperature interval investigated reflects the late stages of ore deposition (Gervilla *et al.* 1996), where crystallization of diarsenides and especially sulfarsenides takes place. In magmatic deposits, these minerals are commonly associated with PGM (Gervilla & Kojonen 2002), and the cobaltite–gersdorffite solid-solution may even contain substantial amounts of PGE (Barkov *et al.* 1999).

Experimental Procedures

Experimental charges of 200 mg were weighed out using pure elements supplied by Alpha Æsar: Fe (Puratronic, 99.995%), Co (Puratronic, 99.995%), Ni (99.997% Ni), As (Puratronic, 99.9999%) and S (Puratronic, 99.9995%). The bulk compositions of the charges were made equal to $(Fe,Co,Ni)As_{1.5}S_{0.5}$. In the experiments at 650°C, 66 charges with different Fe, Co and Ni contents were weighed out, spaced at intervals of 3.33 at.%. The 23 charges examined in the 500°C experiment were placed along the binary joins of the $(Fe,Co,Ni)As_{1.5}S_{0.5}$ plane and along lines corresponding to $(Fe_{0.5}Co_{0.5-x}Ni_x)As_{1.5}S_{0.5}$, $(Fe_{0.65-x}Co_xNi_{0.35})As_{1.5}S_{0.5}$ and $(Fe_{0.3-x}Co_xNi_{0.7})As_{1.5}S_{0.5}$. The sample material was filled into silica tubes, which were sealed under vacuum (0.001–0.005 atm). The charges were heated for prolonged periods (three or four periods of three months); between these annealing intervals, they were reground. The temperatures were controlled using NiCr thermocouples. The temperature gradient within the experimental area of the furnace was found to be ±2.8°C. At the end of the experiment, the charges were quenched in cold water. A LiCl–KCl melt was added to all samples of the 500°C experiment and to selected samples of the 650°C experiment in order to enhance material transport within charge. The addition of the LiCl–KCl melt was done one week before the termination of the experiment, at which point the samples also were reground. This melt was washed out of the samples before sample preparation.

Analytical Methods

The sample material was split in two; one part was prepared as polished sections, and the other investigated by X-ray powder diffraction (PXRD). The polished sections were investigated by means of optical microscopy and electron-microprobe analysis (EMPA).

For some samples, several mineral assemblages were found to be present in each charge. These resulted from the disequilibrium caused by slow rates of reaction and diffusion, as well as the presence of metastable precursor phases. The reported equilibria were established by analyzing the local intergrowths with EMPA and optical microscope. The mineral names ascribed to the different phases are given in accordance to the corresponding natural phase. This correspondence is based on PXRD and EMPA data.

X-ray powder diffraction

Pulverized samples were investigated on a Siemens D5000 diffractometer using Cu$K\alpha$ radiation. The samples were investigated in the 2θ range from 10 to 80°, with the step size of 0.029° and counting time between 2 and 30 seconds depending on the quality of the resulting diffractogram. Data were treated using Brukers EVA program, with subtraction of background and $K\alpha_2$ radiation.

The diffraction peaks from the 650°C experiments are compiled in Figure 1, which shows 2θ *versus* sample number. Identified reflections of each phase are grouped, and we show each phase by a specific color. Values of (*hkl*) are given for each group of peaks. Where peaks overlap, the strongest peaks are shown as overlapping the weaker peaks. The sample numbers are linked to the compositions of the charges, the relation being shown in Figure 1d. They are arranged in series of similar Fe content. The series richest in Fe has 33.3 at.% Fe, the poorest has 0.0 at.%, and the intermediate series are spaced 3.33 at.% apart. The content of (Ni + Co) increases proportionally with the decrease in Fe. Within each series, the increasing sample number corresponds to increasing Ni:Co ratio. The sample richest in (Ni,Fe) in each series lies on the appropriate horizontal dotted line in Figure 1. In this way, it is possible to follow the change in 2θ *versus* those in Fe, Co or Ni. Wherever changes in 2θ with increasing Ni:Co ratio were recognized, they are marked with solid lines. All phases show a general decrease in 2θ with increasing Ni content. Hence, the left-hand side of any field corresponds to the Ni-rich members, and the right-hand side, to the Co-rich members of the solid solution.

The peaks were indexed by comparing them to reference patterns or patterns calculated from structural data by using Powder Cell v. 2.3 (Kraus & Nolze 1999). After indexing, the unit-cell parameters were refined using LCLSQ v. 8.5 (Burnham 1993). The following references to structural descriptions were used to calculate diffraction patterns: skutterudite (Madel & Donahue 1971), cobaltite-*Pa*3 (Giese & Kerr 1965), gersdorffite-*Pa*3 (Bayliss 1968), alloclasite-$P2_1$ (Scott & Nowacki 1976), arsenopyrite-*B*1 (Buerger 1936), löllingite (Kjekshus *et al.* 1974) and pyrrhotite (Fleet 1971, 2*A*3*C* polytype). Alternative structural data are available for arsenopyrite, cobaltite, gersdorffite and löllingite, but the chosen references yielded the best-fitting patterns.

In some cases, it was not possible to unambiguously identify a phase by PXRD or to link certain diffraction peaks to a specific phase. This is caused by the combination of overlapping peaks, in conjunction with variations in the concentrations of phases, as well as the variable composition of some phases within the sample. These problems were most pronounced in the samples from the 500°C experiment, where the large number of 4- and 5-phase equilibria resulted in disequilibrium assemblages of up to eight phases in one sample. Hence, gersdorffite, pyrrhotite and skutterudite were the only phases that could be systematically identified by PXRD in the 500°C experiment. The other phases could only be identified sporadically. The absence of the (010) and (110) reflections and the relative low intensity of the (111) reflection indicate that gersdorffite crystallized in the space group *Pa*3 at both temperatures, and that no As–S ordering occurred. This conclusion was substantiated by the optical isotropism of the synthetic gersdorffite.

The $NiAs_2$ phases encountered in this study could be either rammelsbergite, pararammelsbergite or krutovite. The relevant PXRD data were checked carefully for these phases, but only krutovite could be identified from the 500°C experiments.

Electron-microprobe analysis

Wavelength-dispersion electron-microprobe analyses were performed on a JEOL JCXA–733 Superprobe, using a focused beam. The accelerating voltage was set at 20 kV, and the beam current was 20 nA. The samples were analyzed using Fe$K\alpha$, Co$K\alpha$, Ni$K\alpha$, S$K\alpha$ and As$L\alpha$. Arsenopyrite, pyrite, as well as pure Co and Ni were used as primary standards. Synthetic troilite was used as a secondary standard to correct the analytical data for pyrrhotite.

Experimental Results

The charges were weighed out with a molar ratio of metal to anion equal to 0.5. Therefore, skutterudite should occur in equilibrium with nickeline or pyrrhotite only. This is the case in many samples, although a number of local equilibria involving MX–MX_2 or MX_2–MX_3

FIG. 1. Compilation of the PXRD data of the samples from the 650°C experiments. Each diffraction peak is plotted as a data point. The ordinate gives the sample number, and the abscissa shows the 2θ value of the reflections, where (a) shows the range 10–30°, (b) 30–40° and (c) the range 40–60°. (d) The relation between the bulk composition of the sample and the sample number. The systematic relation between sample number and charge composition divides the samples into series of similar Fe contents, and these are separated by the horizontal dotted lines in Figures 1a to c. Within each series, the Ni:Co ratio increases with increasing sample number. It is thus possible to observe the evolution in peak position as the sample composition changes. If the evolution is caused primarily by a change in the Ni:Co ratio, it gives rise to a number of parallel trends (marked by solid black lines), such as those exhibited by the cobaltite–gersdorffite solid-solution. Peaks of the same reflection are grouped together, and the indices are given by each group. Groups of peaks, which are attributed to the same phase, are given the same color. Strong peaks are shown as overlapping the weaker peaks.

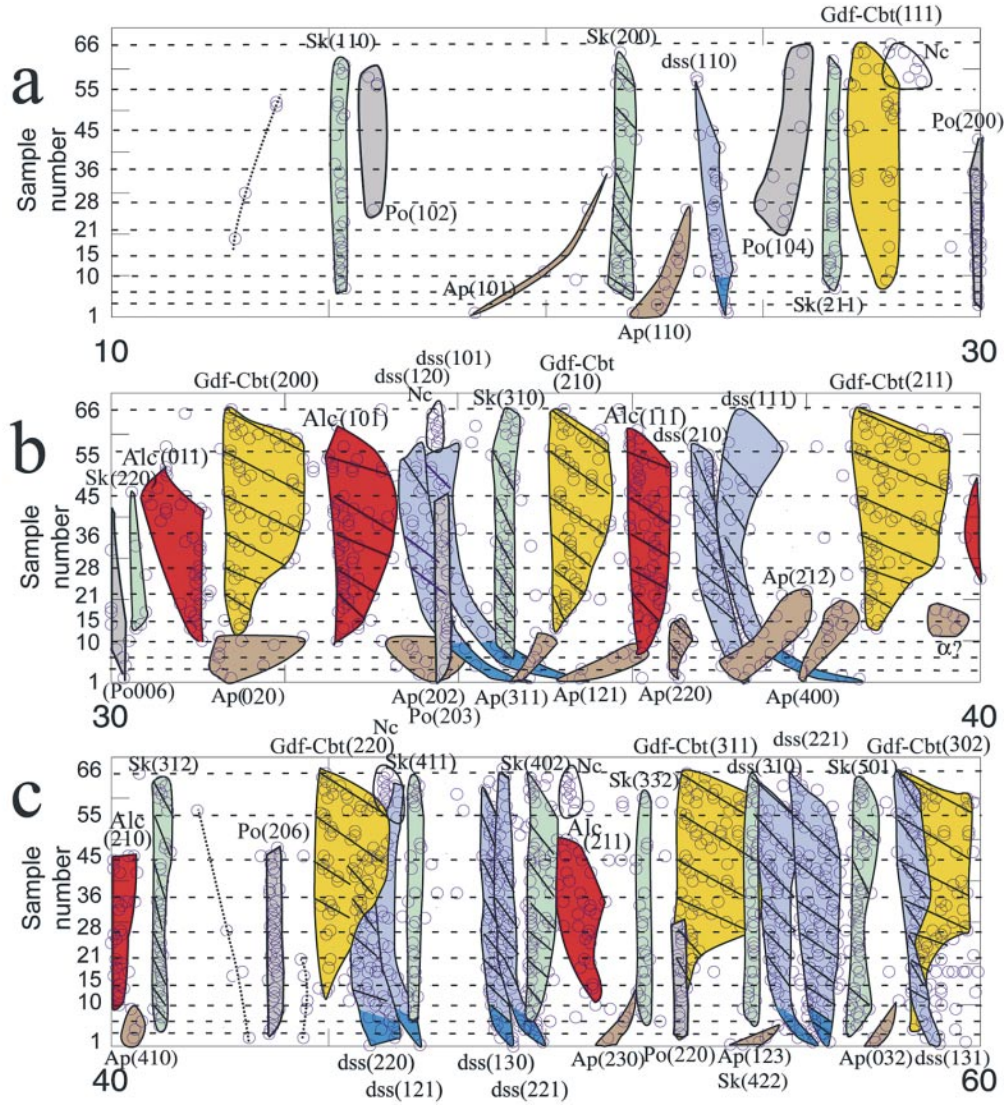
a
Sample number
Sk(110)
Sk(200)
dss(110)
Gdf-Cbt(111)
Nc
Po(200)
Po(102)
Po(104)
Ap(101)
Sk(21H)
Ap(110)
10
30
b
Gdf-Cbt(200)
dss(101)
dss(120)
Nc
Gdf-Cbt
(210)
Sk(310)
Alc(101)
Alc(111)
dss(111)
Gdf-Cbt(211)
Alc(011)
Sk(220)
dss(210)
Ap(212)
α?
(Po006)
Ap(020)
Ap(202)
Po(203)
Ap(311)
Ap(121)
Ap(220)
Ap(400)
30
40
c
Nc
Gdf-Cbt(220)
Gdf-Cbt(311)
dss(221)
Gdf-Cbt(302)
Sk(312)
Sk(411)
Sk(402)
Nc
dss(310)
Sk(501)
Sk(332)
Alc
(210)
Po(206)
Alc
(211)
Ap(410)
dss(220)
dss(121)
dss(130)
dss(221)
Ap(230)
Po(220)
Ap(123)
Sk(422)
Ap(032)
dss(131)
40
60
d
Co 57 58 59 60 61 62 63 64 65 Ni
56 66
46 55
41
37 45
29 36
25
22 28
16 21
13
11 15
7 10
5
4 6
2 3
1 Fe
Sample number and the corresponding position of bulk composition in the MeAsS plane
LEGEND
Skutterudite (Sk)
Pyrrhotite (Po: 2A, 3C polytype)
Alloclasite (Alc)
Gersdorffite - cobaltite (Gdf-Cbt)
Diarsenide solid solution (dss)
Löllingite (Lö)
Krutovite (Krt)
Safflorite (Saf)
Arsenopyrite (Apy) or
αFe0.65Ni0.35As1.4S0.6 (α)
Nickeline
Trend in unidentified peaks

phases have been encountered. Incomplete equilibration was thus the chief obstacle to the determination of the phase relations in this system. The components readily reacted and formed solid phases, but diffusion in the charges was inadequate to lead to proper equilibration. Addition of LiCl–KCl melt and repeated grinding reduced this problem without eliminating it entirely. This partial equilibrium resulted in two main problems: (1) the presence of disequilibrium or of several phase associations in the same charge, and (2) variation in phase composition in a given assemblage in one charge. The first problem was countered in part by analyzing selected aggregates from each charge, which were chosen according to textural criteria. More often than not, samples localized close to the boundary between two phase-assemblage volumes contained aggregates representing phases from both phase assemblages. In such cases, samples lying further away from the phase-volume boundary revealed the true assemblage, and choosing them helped us to interpret the more complicated cases. The problem of intra-charge compositional variation of phases from similar associations was countered by calculating selected average compositions.

It is possible to categorize the observed phase-equilibria according to the variance they show, by using the phase rule ($f = c + 2 - p$). There are five components present, and the pressure equals the vapor pressure of constituents. The sum of the variance and the number of phases ($f + p$) is thus seven. For most temperature levels selected, the observed phase-assemblage is stable in a temperature *interval*: $f \geq 1$. This gives the maximum number of phases as six, *i.e.*, five phases in addition to the vapor. Where the *M*:*X* ratio of all involved phases is 0.5, the system behaves like a quaternary system, as it makes the concentration of any one element dependent on the concentration of the other four. This reduces the variance, and hence the maximum number of phases, by one. The observed equilibria are thus univariant, divariant, trivariant or tetravariant corresponding to a quaternary assemblage of 4, 3, 2 or 1 phases in addition to vapor. The univariant equilibrium consists of four solid phases of fixed composition. The three phases of the divariant equilibria display compositions that lie on three interrelated compositional trends. The trivariant equilibria occur as two coexisting fields, whereas the tetravariant equilibrium corresponds to a single phase. The system behaves like a five-component system if the *M*:*X* ratio of the involved phases deviates from 0.5, in which case one phase is added, so that a two phase-assemblage exhibits tetravariance, *etc.* Table 3 summarizes the observed equilibria according to the number of phases. Nickeline, jaipurite and langisite occur in disequilbrium assemblages overgrown by gersdorffite, cobaltite, alloclasite or skutterudite. Langisite and jaipurite only appeared in the 500°C ex-

TABLE 3. PHASE EQUILIBRIA FORMED IN THE $(Fe,Co,Ni)As_{1.5}S_{0.5}$ PLANE OF THE SYSTEM Fe–Co–Ni–As–S

univariant	divariant	trivariant	tetravariant
	650°C isothermal section		
Alc + α + *dss* + Sk + Po	α + *dss* + Sk + Po	*dss* + Sk + Po	Alc
	α + Alc + *dss*	Gdf + *dss*	*dss* + Sk
	Alc + *dss* + Sk + Po	Apy + Lö	Gdf + Nc
	Alc + *dss* + Gdf	Apy + Sk + Po	Apy + Po
	Apy + Lö + Sk + Po	Alc + *dss*	Sk + Gdf
	Alc + Gdf + Sk + Po	Gdf + Krt	
		α + *dss*	
		Alc + Gdf	
	500°C isothermal section		
Saf + Lö + Krt + Sk + Po	*dss* + Gdf + Sk + Po	Saf + Sk + Po	Saf
Saf + Gdf + Krt + Sk + Po	*dss* + Gdf + Krt	Saf + Gdf + Krt	Apy
dss + Gdf + Krt + Sk + Po	Apy + Lö + Sk + Po	Gdf + Krt	Gdf + Nc
Apy + *dss* + Lö + Sk + Po	Apy + *dss* + Sk + Po	*dss* + Gdf	Alc + CoAs
Apy + *dss* + Gdf + Sk + Po	Apy + *dss* + Lö	Apy + Lö	Alc + CoS
Alc + Saf + Gdf + Sk + Po	Alc + Saf + Sk + Po	Apy + *dss*	dss + Sk
	Alc + Saf + Gdf	Alc + Sk + Po	Sk + Gdf
		Alc + Saf	
		Alc + Gdf	
		Alc + Cbt	

Symbols: Alc: alloclasite, Apy: arsenopyrite, Cbt: almost stoichiometric cobaltite, Gdf: any member of the gersdorffite–cobaltite solid-solution, Lö: löllingite, Nc: nickeline, Po: pyrrhotite, Krt: krutovite, Sk: skutterudite, Saf: safflorite, *dss*: diarsenide solid-solution, α: unknown sulfarsenide. Vapor is present in all assemblages.

periments. Data are presented and discussed as atom percent or as atoms per formula unit (*apfu*).

The intersections of skutterudite – pyrrhotite tielines with the MX_2 plane

A systematic presentation of data on the phase relations in the system (Fe,Co,Ni)(As,S)$_2$ meets with the obstacle of compressing five-component data into a three-dimensional scheme. The maximum number of parameters that can be shown in a non-interactive medium is four, as in a tetrahedral plot or a trigonal prism. This number can be increased by presenting the same data in several figures, but it requires that each data point can be identified in all figures. A trigonal prism with a base consisting of a Fe–Co–Ni triangle and a virtual *y*-axis displaying the arsenic content can be used in cases where there is little overlap in the metal distribution of the phases shown. The virtual *y*-axis is presented as values ascribed to the data points. This presentation is equivocal if the sum of arsenic and sulfur varies relative to the sum of metals. This is the case where *MX* and MX_3 phases participate in the equilibria. To address this problem, the chemical coordinate of the intersection between the *MX*–MX_3 tieline and the MX_2 plane was calculated, thereby allowing projection of their compositions into the MX_2 prism. The chemical coordinate can be calculated if the ratio of skutterudite to pyrrhotite is known. The intersection is defined by having a composition equal to MX_2, so the equation describing the relation between the intersection coordinate and the compositions of skutterudite and pyrrhotite is: 1) $MX_2 \Leftrightarrow a\ MX_3 + b\ MX$. Any MX_2 phase formed in equilibrium with skutterudite and pyrrhotite can be left out of the equation, as it would not affect the ratio of skutterudite to pyrrhotite. However, pyrrhotite contains a lower proportion of metal, and skutterudite contains less arsenic, than implied by the *MX* and MX_3 formulas, so it is necessary to write the equation as 2) $MX_2 \Leftrightarrow a\ MX_{3-X} + b\ M_{1-Y}X$, where *Y* is the metal deficit in pyrrhotite, and *X* the arsenic deficit in skutterudite. In terms of atom percent, this reaction equals 3) $M_{33.33}X_{66.67} \Leftrightarrow a\ M_{25+X}X_{75-X} + b\ M_{50-Y}X_{50+Y}$. This equation can then be solved for either metals or anions by combining with ($a + b = 1 \Leftrightarrow b = 1 - a$), yielding 4) $a = (16.67 - Y) / [25 - (X + Y)]$. Thus, the exact chemical coordinate of the intersection was calculated as a weighted average based on the values of *a* and *b,* which yielded average compositions in the range (Fe,Co,Ni) $As_{1.38–1.42}S_{0.62–0.58}$. Figure 2 displays the calculated intersections and the average compositions on which the intersections are based (from the 650°C isotherm).

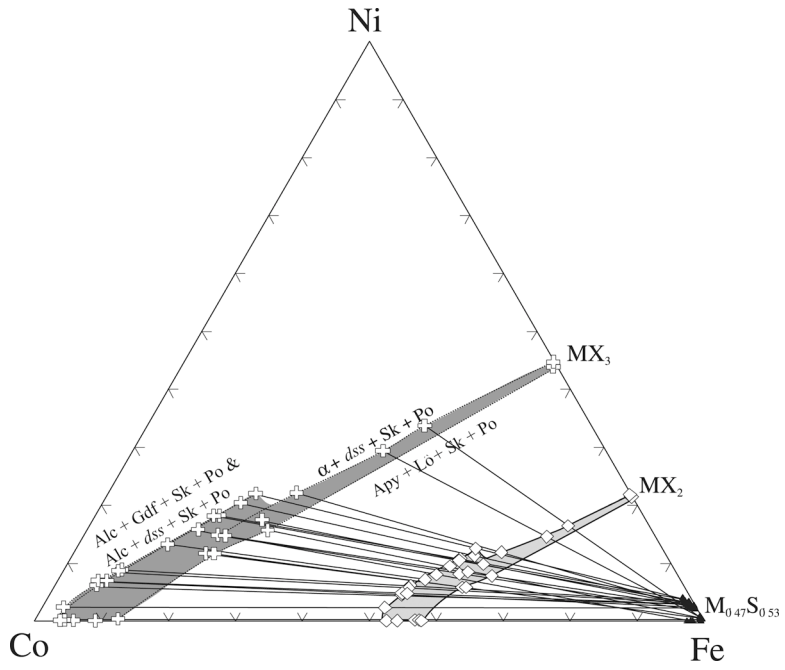

FIG. 2. The skutterudite–pyrrhotite pair in coexistence with MeX_2 phases. The average composition of skutterudite (dark grey field, white crosses) and pyrrhotite (black triangles) from different assemblages is indicated, as well as the calculated intersections (light grey) of the Sk–Po tieline with the MeX_2 plane. The dotted lines show the compositions of skutterudite from different divariant phase-assemblages.

THE 650°C EXPERIMENTS

The diarsenide solid-solution (*dss*) dominates the phase relations at 650°C, although alloclasite (Alc), gersdorffite (Gdf), löllingite (Lö) and skutterudite (Sk) also exhibit extensive solid-solutions. The *dss* field coexists with alloclasite, arsenopyrite, gersdorffite, $\alpha Fe_{0.65}Ni_{0.35}As_{1.4}S_{0.6}$ (α) or skutterudite and pyrrhotite (Po). The phase called $\alpha Fe_{0.65}Ni_{0.35}As_{1.4}S_{0.6}$ occurs as a semicircular solid-solution field centered upon $(Fe_{0.65}Ni_{0.35})As_{1.4}S_{0.6}$. It has an PXRD pattern related to that of arsenopyrite, and there is an irregular, partially bimodal evolution in 2θ values from arsenopyrite to $\alpha Fe_{0.65}Ni_{0.35}As_{1.4}S_{0.6}$. This evolution could be the result of overlap between arsenopyrite and $\alpha Fe_{0.65}Ni_{0.35}As_{1.4}S_{0.6}$ in changing proportions, or it could suggest that both phases were members of the same solid-solution series. For example, the $\alpha(Fe_{0.65}Ni_{0.35})As_{1.4}S_{0.6}$ phase may be a continuation of the arsenopyrite solid-solution, which runs through a sulfur-enriched area with respect to those investigated during the experiments. Hypothetically, arsenopyrite from the Apy + Sk + Po assemblage could bridge the gap between Apy and α, and this phase volume would exist in more sulfur-enriched environments than those investigated.

Whether löllingite and *dss* are two separate phases cannot be shown, as they were not found in equilibrium with each other, but the PXRD data suggest that they are. The trend of some of the 2θ values changes drastically when moving from löllingite toward *dss*, whereas they change little throughout the extensive *dss* solid-solution field (Fig. 1). The composition of the coexisting phases are listed in Appendix A according to sample number and phase relations. Appendices A and B are available from the Depository of Unpublished Data, CISTI, National Resarch Council of Canada, Ottawa, Ontario K1A 0S2, Canada.

DESCRIPTION OF PHASES FORMED AT 650°C

Alloclasite

Alloclasite exhibits extensive solid-solution with regard to both Fe – Co – Ni proportions and As:S ratio (Figs. 3, 4). Alloclasite coexists with all phases in the system except for arsenopyrite, löllingite and rammelsbergite. The arsenic-rich boundary of the alloclasite chemical volume coexists with the diarsenide solid-solution, and the sulfur-rich boundary coexists with gersdorffite or skutterudite and pyrrhotite. The As content varies from 37 to 54 at.% depending on the mineral assemblage and Fe–Ni content. Cobalt can be completely replaced by a mixture of Fe and Ni. The unit cell

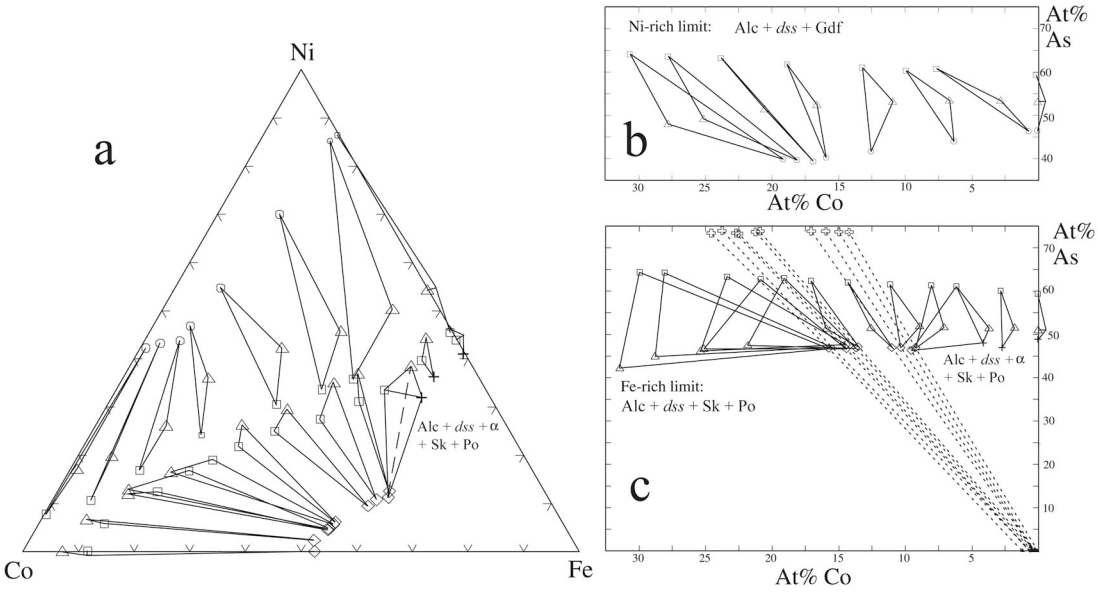

FIG. 3. Compositions of alloclasite and phases coexisting with the Ni-rich and Fe-rich limits of the alloclasite solid-solution, which define the limit of the As-rich top of the alloclasite solid-solution. (a) Fe–Co–Ni plot of both the Alc + *dss* + Gdf and the Alc + *dss* + Sk + Po assemblages. (b) The Co *versus* As plot of Alc + *dss* + Gdf assemblage. (c) The Co *versus* As plot of Alc + *dss* + Sk + Po assemblage. Traces of the Sk + Po tieline are shown with dotted lines. Their intersection with the MeX_2 plane is shown by diamonds. Alloclasite is indicated by triangles, diarsenide by rectangles, gersdorffite as circles, pyrrhotite as filled triangles, α as crosses, and skutterudite as open crosses.

of Co-free alloclasite (sample 28; 15.5 at.% Fe, 18.5% Ni, 12.8% S and 53.2% As, measured by EMPA) was refined in space group $P2_1$ to *a* 4.868(7), *b* 5.778(5), and *c* 3.318(6) Å based on 11 reflections. The (100) reflection is lacking. Kingston (1971) reported that the (*h*00) reflections are missing from alloclasite synthesized at 700°C. The reported diffractogram is similar to that of alloclasite from this study. Kingston (1971) suggested that the synthetic alloclasite crystallized in space group $P22_12_1$.

The Fe-rich limit of the alloclasite solid-solution coexists with diarsenide and the phase $\alpha(Fe_{0.65}Ni_{0.35})As_{1.4}S_{0.6}$ (Fig. 3). The three phases can coexist until the assemblage contains more than 3.7 at.% Co. At this point, the $\alpha(Fe_{0.65}Ni_{0.35})As_{1.4}S_{0.6}$ phase is saturated with Co, and the stable assemblage is alloclasite, *dss*, $\alpha(Fe_{0.65}Ni_{0.35})As_{1.4}S_{0.6}$, skutterudite and pyrrhotite. Adding further Co removes $\alpha(Fe_{0.65}Ni_{0.35})As_{1.4}S_{0.6}$ from the assemblage, and alloclasite, *dss*, skutterudite and pyrrhotite coexist until the Co–Fe join is reached. At this point, the alloclasite contains 2.4 at.% Fe.

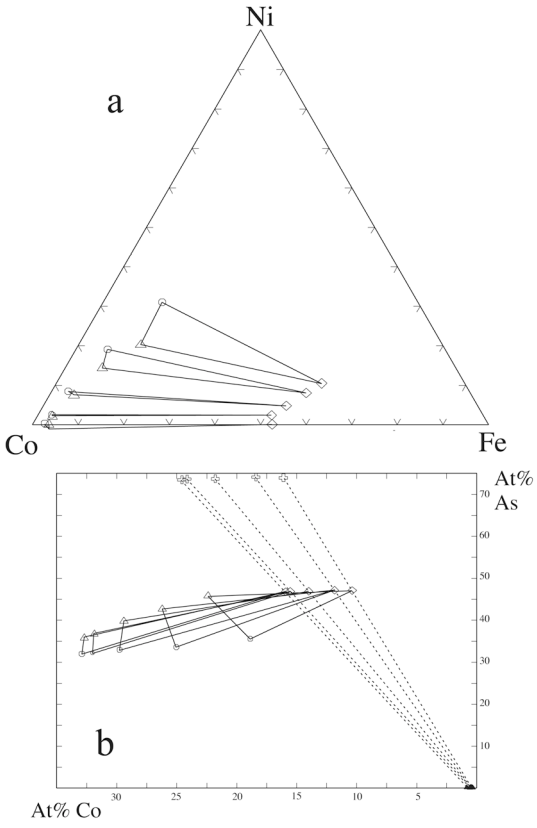

FIG. 4. Compositions of coexisting alloclasite, cobaltite–gersdorffite, skutterudite and pyrrhotite. (a) Fe – Co – Ni distribution. (b) Co *versus* As plot. The symbols are the same as in Figure 2.

The Ni-rich limit of alloclasite is defined by the equilibria between alloclasite, gersdorffite and *dss* (Fig. 3). Along this line, compositions range from $(Co_{0.85}Ni_{0.15})As_{1.47}S_{0.53}$ to $(Fe_{0.45}Ni_{0.55})As_{1.61}S_{0.39}$. Starting at the Co–Ni join, the compositions of alloclasite form a smooth curve of increasing at.% Ni and at.% Fe values and As contents until approximately 0.51 *apfu* Co has been exchanged for Fe and Ni. At this point, the curve breaks and forms a nearly straight line to the Fe–Ni join.

The S-rich limit of alloclasite is found in mineral assemblages containing gersdorffite, skutterudite and pyrrhotite (Fig. 4). This phase assemblage is only found as local equilibria in Co-rich samples and is invariably overgrown by more As-rich assemblages. Alloclasite from this assemblage has a composition in the range $Fe_{0.03}Co_{0.97}As_{1.09}S_{0.91}$ to $Fe_{0.15}Co_{0.64}Ni_{0.21}As_{1.39}S_{0.61}$.

Arsenopyrite

Arsenopyrite solid-solution contains up to 1.6 at.% Ni, 11% Co and 40% As, and is limited compared to the extensive solid-solutions exhibited by the other sulfarsenides. There is no systematic correlation between the metal contents and the As–S contents.

The As-rich side is defined by the equilibrium with löllingite; toward Co–Ni, it is limited by the association of Apy + Lö + Sk + Po. The compositions of the Apy + Lö + Sk + Po assemblages are displayed in Figure 5.

$\alpha(Fe_{0.65}Ni_{0.35})As_{1.4}S_{0.6}$

This phase is found coexisting with *dss* and any or all of alloclasite, skutterudite and pyrrhotite. Its solid solution is a field centered on $Fe_{0.65}Ni_{0.35}As_{1.40}S_{0.60}$, with an extent of 0.06–0.09 *apfu* toward Fe, Co and Ni. The As contents vary from 1.32 to 1.48 *apfu*, although in disequilibrium occurrences, As contents as low as 1.14 *apfu* were found. The As contents increase with increasing Ni contents. Figure 6 shows the compositions of $\alpha Fe_{0.65}Ni_{0.35}As_{1.4}S_{0.6}$ coexisting with the above-mentioned phases. This phase could either represent a continuation of the arsenopyrite solid-solution toward higher Ni and As contents, separated from arsenopyrite of the skutterudite + pyrrhotite coexistence, or it could be a separate phase with a structure closely related to that of arsenopyrite. The PXRD data (Fig. 1) yield no clear answers to this question, as overlap between the peaks of α and arsenopyrite could produce the observed changes. The large and partially bimodal variation in the Apy (301) peak suggests that two different phases are present, as does the presence of an unidentified peak with 2θ in the range 39.6–39.8° (marked α? in Fig. 1).

Cobaltite – gersdorffite solid-solution

There is seemingly a complete solid-solution between cobaltite and gersdorffite (Figs. 3, 4). The As content along this solid-solution series correlates lin-

early with the Ni content. The Co end-member has a composition very close to CoAsS, whereas the Ni end-member contains 50 at.% As. Ni-rich members of this series contain up to 7 at.% Fe, and there is a negative correlation between Fe and As contents. Cobaltite–gersdorffite is found coexisisting with alloclasite, *dss*, pyrrhotite, skutterudite or krutovite. The limit of the Fe-rich side of this solid solution was not established, as it extends toward compositions richer in sulfur than those investigated. Klemm (1965a) found that it contains up to approximately 22 at.% Fe where it coexists with arsenopyrite at 650°C.

The unit-cell parameter *a* varies from 5.566(3) to 5.708(2) Å in going from the Co to the Ni end-member. Strong covariance among Ni, As and Fe makes it impossible to statistically estimate the impact of each element on the cell constant. The standard deviations of the unit-cell refinements increase toward the region between 5.61 and 5.65 Å. In this range, no data are present, out of 35 sample points. In our opinion, the solid-solution is composed of two separate phases of closely related composition and structure.

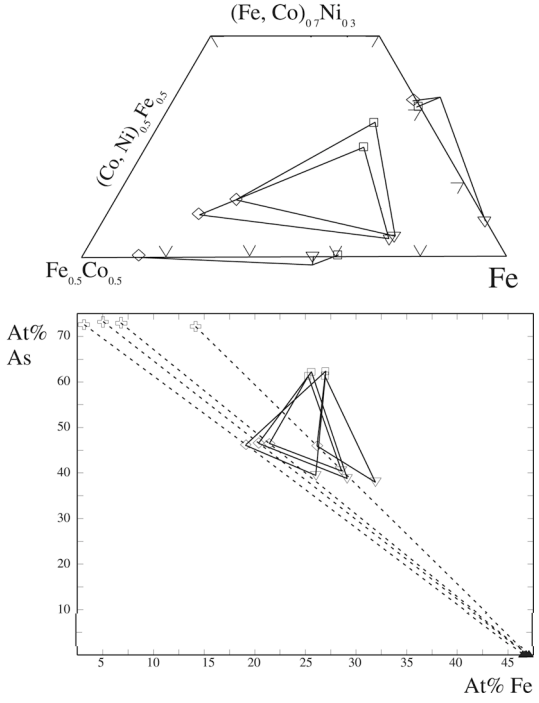

FIG. 5. Compositions of arsenopyrite coexisting with löllingite, skutterudite and pyrrhotite. Arsenopyrite is indicated by triangles, löllingite as squares, and the intersection of skutterudite–pyrrhotite by diamonds.

Diarsenide solid-solution (*dss*)

In the assemblages investigated, this phase covers a range of compositions, between the extremes $CoAs_{1.82}S_{0.18}$, $(Fe_{0.13}Co_{0.28}Ni_{0.63})As_{1.73}S_{0.27}$ and $(Fe_{0.70}Ni_{0.30})As_{1.92}S_{0.08}$ (Fig. 7). Ni-rich members contain less As, whereas members richer in Fe and Co have higher As contents. The phase *dss* coexists with all other phases in the system except krutovite and löllingite. The area of the *dss* field richer in Fe and Ni is connected to the Co-rich area by few compositions forming a thin sliver, as indicated by the question mark in Figure 7. This area could indicate the presence of two phases close in composition, safflorite on the Co-rich side, and *dss* on the Fe–Ni-rich side. The Ni- and Fe-rich limits of *dss* were not established, probably because the limiting phase volumes have compositions richer in As than those investigated. The unit cell of *dss* (3.9 at.% Fe, 30.0% Co, 0.01% Ni, 1.7% S and 64.3% As) was refined in space

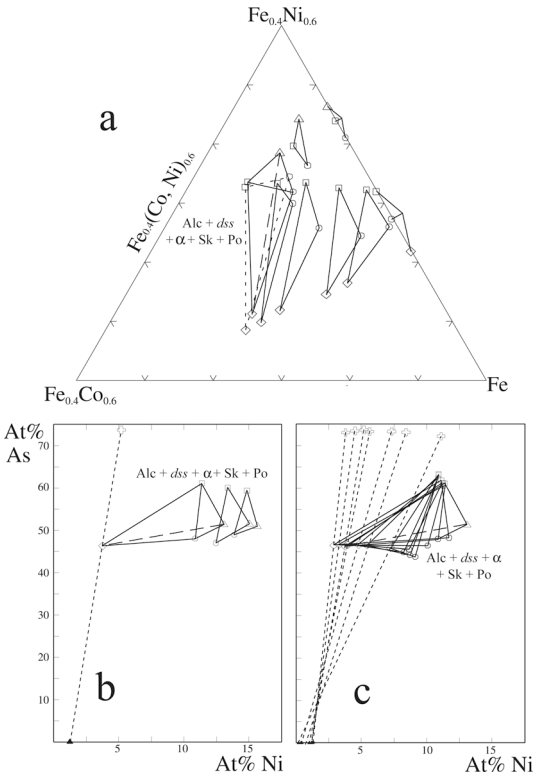

FIG. 6. The equilibria involving the $\alpha(Fe_{0.65}Ni_{0.35})As_{1.4}S_{0.6}$ solid-solution field. For Ni-rich compositions, this solid solution is limited by the assemblage of Alc + *dss* + α; toward Co and Fe, it is limited by the *dss* + α + Sk + Po assemblage. These meet in the Alc + *dss* + α + Sk + Po association. Phase α is shown by circles, otherwise the notation is as in Figure 3.

group *Pnnm*: *a* 5.17(2), *b* 5.82(4), *c* 3.01(3) Å, on the basis of seven reflections.

Löllingite and krutovite

A nickel diarsenide containing up to 1 at.% Co or Fe and 12–14 at.% S was found to coexist with gersdorffite. It was not possible to identify it by optical microscopy or X-ray diffraction, possibly because of the very low concentration of the Ni diarsenide. The phase in question may be either krutovite, pararammelsbergite or rammelsbergite.

The anisotropic rammelsbergite or pararammelsbergite should be easily discernible from gersdorffite in reflected light microscopy. As they seem to be absent, the phase in question may be krutovite. The $NiAs_{2-X}S_X$ phase present contains much more sulfur than the rammelsbergite synthesized at 600° and 700°C by Yund (1962). Instead, the $NiAs_{2-X}S_X$ phase ($0.25 < X < 0.29$) corresponds to members of the gersdorffite solid-solution series, as reported by Yund. This leaves two possibilities: 1) Yund is correct, and this phase is simply a member of the gersdorffite solid-solution, existing owing to the imperfect equilibrium. This is contrary to the systematic coexistence of the $NiAs_{2-X}S_X$ phase and gersdorffite with a composition within the range $(Ni_{0.95\pm0.05}Co_{0.05\pm0.05}Fe_{0.02\pm0.01})As_{1.54\pm0.03}S_{0.46\pm0.03}$. 2) The $NiAs_{2-X}S_X$ phase is in fact distinct from gersdorffite, most likely krutovite. Krutovite occurs in very low abundance in samples completely dominated by gersdorffite, and because it is optically similar to and homeotypic with gersdorffite, it could have been overlooked during microscopy and PXRD.

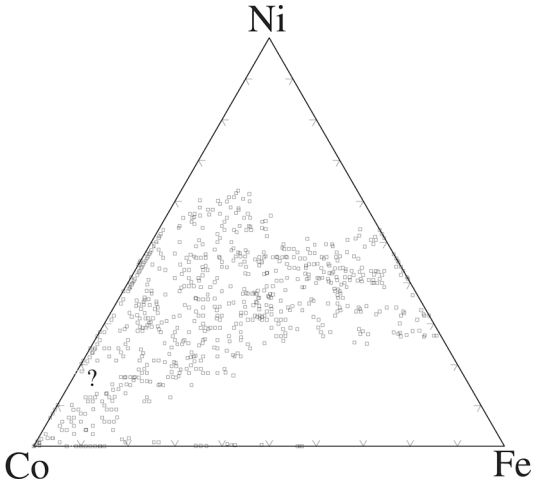

FIG. 7. Compositions of diarsenide solid-solution (*dss*) as found by EMPA. The Fe–Ni-richer area of the *dss* field is connected to the Co-rich area by few analyses forming a thin sliver near the question mark. This area could indicate two phases close in composition. Safflorite on the Co-rich side, and *dss* on the Fe–Ni-rich side.

Löllingite contains up to 11 at.% Co or Ni and between 61 and 65 at.% As. High Fe contents favor low S contents. It occurs in equilibrium with arsenopyrite or skutterudite and pyrrhotite. The unit-cell parameters of löllingite (29.6 at.% Fe, 0.0% Co, 3.9% Ni, 4.0% S and 62.5% As) were refined in the space group *Pnnm*: *a* 5.251(1), *b* 5.961(1) and *c* 2.890(3) Å, on the basis of 17 reflections.

Skutterudite

The triarsenides of Fe, Co and Ni display a complete solid-solution between skutterudite ($CoAs_3$) and $(Fe,Ni)As_3$. For the assemblages observed, the solubility of Fe and Ni is limited to the central portions of the system, slightly below the Ni : Fe = 1 : 1 ratio (Fig. 2). The As content varies from 72 to 74 at.%. This variation can in part be attributed to the substitution of As by S (0.8 to 2.5 at.%). There is a negative correlation beween the As and the S contents and a significant, albeit limited, variation in *Me*, the metal content (24.9 to 26.1 at.%). The highest metal content is found in skutterudite containing 73.4 at.% As, and the maximum metal content decreases both toward higher and lower As contents (Fig. 8). The decrease toward lower As contents is caused by the S-for-As substitution, the decrease toward higher As probably reflects nonstoichiometry. There is a connection between metal content *versus* As relation and phase-assemblage (Fig. 8), supporting the assumption that the observed nonstoichiometry is an aspect of phase equilibria and the crystal chemistry of skutterudite, and not an analytical artefact. This phenomenon has been reported earlier by Roseboom (1962), Klemm (1965b) and Petruk *et al.* (1971). The latter found the *Me*:*X* ratio in skutterudite to vary from 1:2.60 to 1:2.93. The *Me*:*X* ratio in skutterudite from this study varies from 1:2.84 to 1:3.02. One possible reason for the very low values found by Petruk *et al*. (1971) is that they did not analyze for sulfur, and any substitution of As by S would thus contribute to a falsely lowered ratio. Skutterudite-type antimonide and phosphide phases have been synthesized for materials research (among others Sales *et al.* 1997, Bauer *et al.* 2000). In these materials, it was possible to stuff a large cation into the icosahedral site located in the center of the unit cell, thereby changing the general formula to $A_{0-1}Me_4X_{12}$. This formula corresponds to a minimum cation : anion ratio of 1 : 2.4. If similar filling occurs in the present phases, it would explain the observed nonstoichiometry.

The unit-cell size of skutterudite varies from 8.186(5) to 8.236(1) Å in going from almost pure skutterudite to the Fe–Ni-substituted skutterudite.There is a strong interdependence among Co, Fe and Ni, as well as a limited variation in the As, S and *Me* contents,

making it impossible to statistically evaluate the impact of each element on unit-cell size.

Pyrrhotite

Pyrrhotite displays limited solid-solution; from 44.1 to 48.1 at.% Fe, 0–1.2% Co, 0–2.0% Ni, 0– 0.14% As, and from 51.8 to 53.8% S. There is some compositional overlap between pyrrhotite from different assemblages (Fig. 9), probably caused by a combination of analytical and experimental uncertainty. The As content varies irrespective of phase assemblages, and is most likely the result of analyses made on pyrrhotite with an admixture of any of the As-bearing phases.

The Ni content of pyrrhotite forms two clear groups, one with 1 to 2 at.% Ni and one with 0.5 to 0 at.% Ni (Fig. 9). Pyrrhotite belonging to the Ni-poor group is found in mineral assemblages containing löllingite or arsenopyrite. The other phase-assemblages contain pyrrhotite from both groups except the Alc + *dss* + Sk + Po assemblage, which only contains Ni-rich pyrrhotite. Numerous investigators have reported complete solid-solution between FeS and NiS at this temperature, which suggests that the observed solid-solution gap just shows different members of the same phase.

There is litle variation in the unit-cell size; the *d*(102) reflection is almost constant and varies from 2.062 to 2.074 Å, with an average of 2.068(3) Å. It corresponds to a minimum subcell volume of 58.7(1) Å^3 (*a* 3.442(3), *c* 5.72(1) Å; 45.1 at.% Fe, 0.4% Co, 1.6% Ni, 52.7% S, 0.0% As) and a maximum volume of 59.31(6) Å^3 (*a* 3.449(1), *c* 5.756(6) Å; 47.5 at.% Fe, 0.3% Co, 0.0% Ni, 52.2% S, 0.1% As).

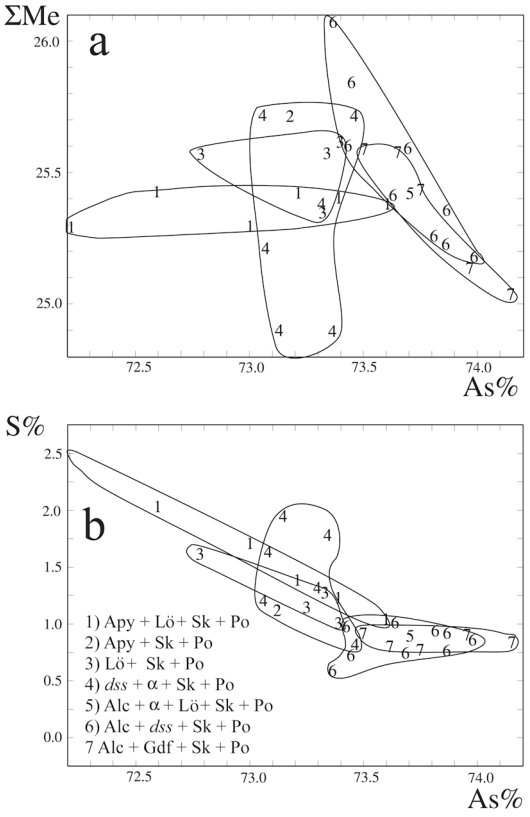

FIG. 8. (a) *Me* – As plot showing the compositions of skutterudite from different assemblages. (b) As *versus* S plot showing the extent of the S-for-As substitution in skutterudite. Skutterudite compositions deviate from MeX_3 stoichiometry by as much as 1 at.%, corresponding to the formula $MeX_{2.84}$. This phenomenon has been reported from natural and synthetic samples of skutterudite (Petruk *et al.* 1971, Roseboom 1962).

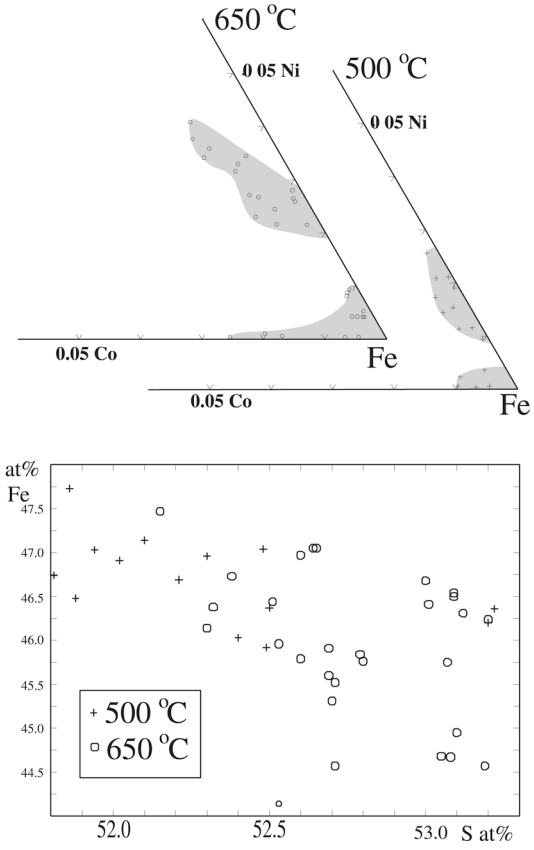

FIG. 9. Compositions of pyrrhotite formed at 650° and 500°C. The Fe–Co–Ni contents generally reflect the overall composition of the phase assemblage, but there is large overlap between pyrrhotite from the different parageneses.

The (Fe,Co,Ni)(As,S)$_2$ prism at 650°C

The phases presented in the foregoing sections all are located in the As-rich area of the compositional volume defined by the (Fe,Co,Ni)(As,S)$_2$ prism. They are compiled in Figures 10, 11, 12 and 13. Compositional data indicated in these figures were recalculated to formula units, based on $\Sigma X = 2$. The phases are colored according to the legend given in Figure 1. Figure 10 shows the composition of löllingite, *dss* and krutovite coexisting with alloclasite, $\alpha(Fe_{0.65}Ni_{0.35})As_{1.4}S_{0.6}$, arsenopyrite, gersdorffite, skutterudite and pyrrhotite. The fields shown in Figure 10 correspond to the As-poor sides of the solid-solution volumes of diarsenides, and Figure 11 shows the As-rich limits of the phases coexisting with the diarsenides from Figure 10. In both these figures, the As contents of the phases are indicated at the data points, as are the phase assemblages. In addition to vapor, each data point in Figure 10 coexists with one (trivariant assemblage), two (divariant), or three data points (univariant) in Figure 11. The divariant assemblages are marked with solid lines, which separate the trivariant fields. As the imaginary tielines between the figures do not cross each other, it is possible to navigate between them, by counting the charges from the edges of the solid-solution fields. The Ni-rich parts of the *dss* field coexist with gersdorffite (Fig. 10). The Ni limit of the *dss* field was not encountered during this experiment; it is probably defined by the *dss* + Gdf + Krt equilibria, and it would require charges richer in As

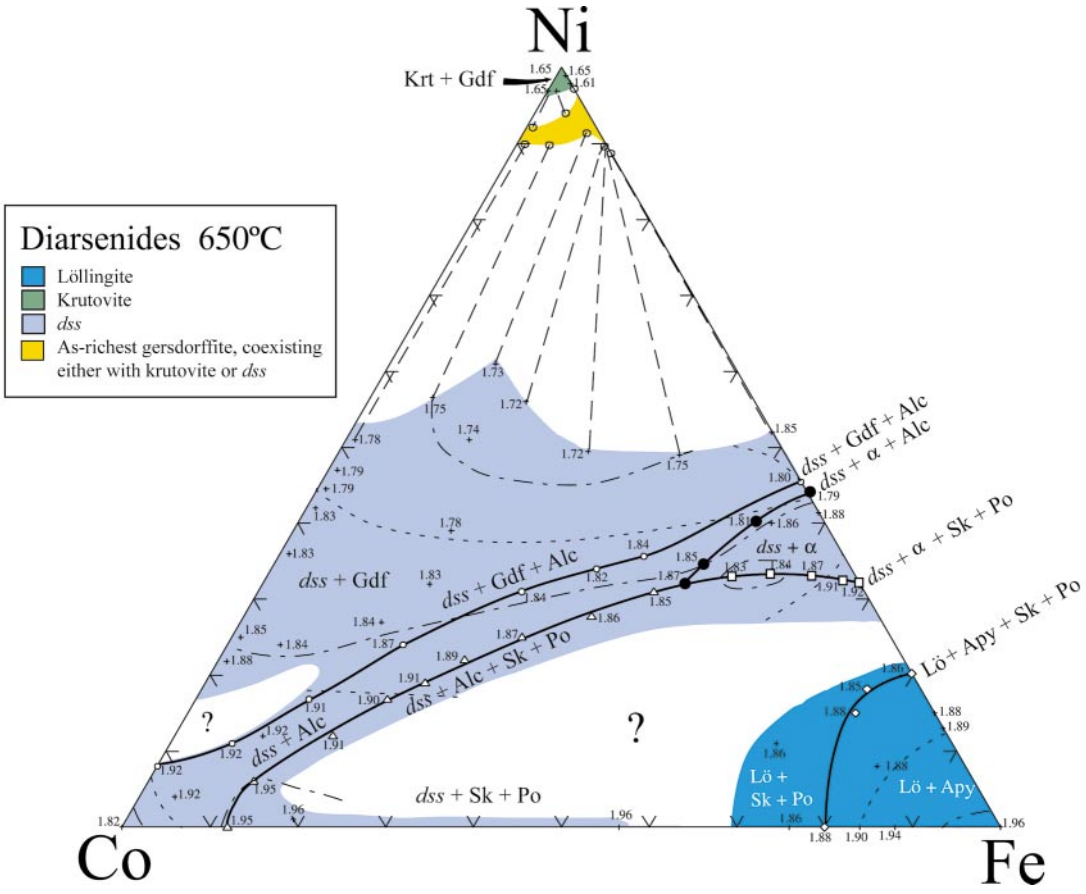

FIG. 10. Diarsenides formed at 650°C in equilibrium with sulfarsenides or skutterudite and pyrrhotite. The solid-solution field shown corresponds to the As-poor side of the diarsenide solid-solution volume. The solid-solution fields are divided into subareas according to phase assemblage. The solid lines represent diarsenide compositions from the divariant assemblages. The data points show compositions from Appendix A (deposited), with As contents (in *apfu*) indicated. The contour lines, obtained by inter- and extrapolation between the data points, display the variation in As content throughout the field in intervals of 0.05 *apfu*. This figure connects with Figure11, which shows the coexisiting sulfarsenides. Question marks indicate areas where no compositions were found or where the phase equilibria were not determined. Phase abbreviations are those used in Table 3; colors correspond to the legend in Figure 1.

to be delineated. Gersdorffite compositions with which the *dss* richest in Ni coexists are plotted, in order to establish the connection between Figures 10 and 11.

The most prominent feature of Figure 11 are the large solid-solution fields of alloclasite and cobaltite–gersdorffite. Close to the Co corner, the As content of alloclasite coexisting with *dss* becomes a function of Fe content, rather than of Ni content as elsewhere. This could be an indication of an as yet unrecognized change in phase assemblage, *e.g.*, *dss* and safflorite may be two distinct phases, although of very similar composition.

Figure 12 shows the composition of coexisting alloclasite, cobaltite–gersdorffite, skutterudite and pyrrhotite. The As-rich side of the cobaltite–gersdorffite solid-solution is shown and the inset figure shows the As-poor side of alloclasite coexisting with it. This assemblage is substantially poorer in As than the bulk composition, and it was only found as local equilibria, located inside the field of skutterudite. This is the reason why this portion the diagram was incompletely investigated. The cobaltite and arsenopyrite solid-solutions as determined by Klemm (1965a) are included in Figure 12. Klemm's data show the compositional limits of coexisting arsenopyrite and cobaltite; both are, supposedly, located in the *Me*AsS plane. Hypothetically, Klemm's solid-solution limits could represent the continuation of the cobaltite–gersdorffite and the arsenopyrite solid-solution fields toward compositions richer in S. The sides of the $(Fe,Co,Ni)(As,S)_2$ prism, presented as $(Fe, Ni)(As,S)_2$, $(Fe,Co)(As,S)_2$ and $(Co,Ni)(As,S)_2$ diagrams, are shown in Figure 13. These diagrams interconnect Figures 10, 11 and 12.

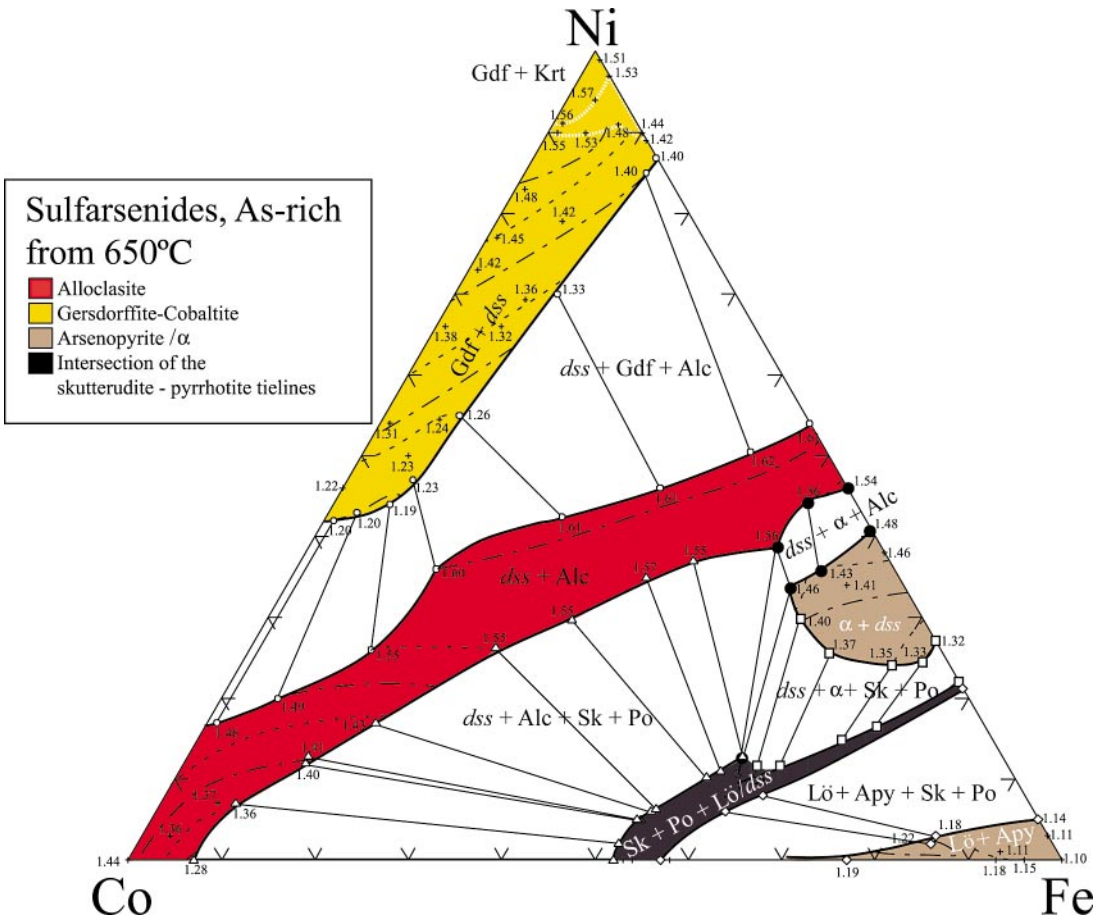

FIG. 11. Sulfarsenides formed at 650°C in equilibrium with diarsenides or skutterudite and pyrrhotite. The solid-solution fields shown describe the As-rich side of the sulfarsenide solid-solution volumes. The intersection of the skutterudite–pyrrhotite tielines with the MeX_2 prism form the black field; they intersect at roughly 1.41 *apfu* As. Other notations correspond to those in Figure 10.

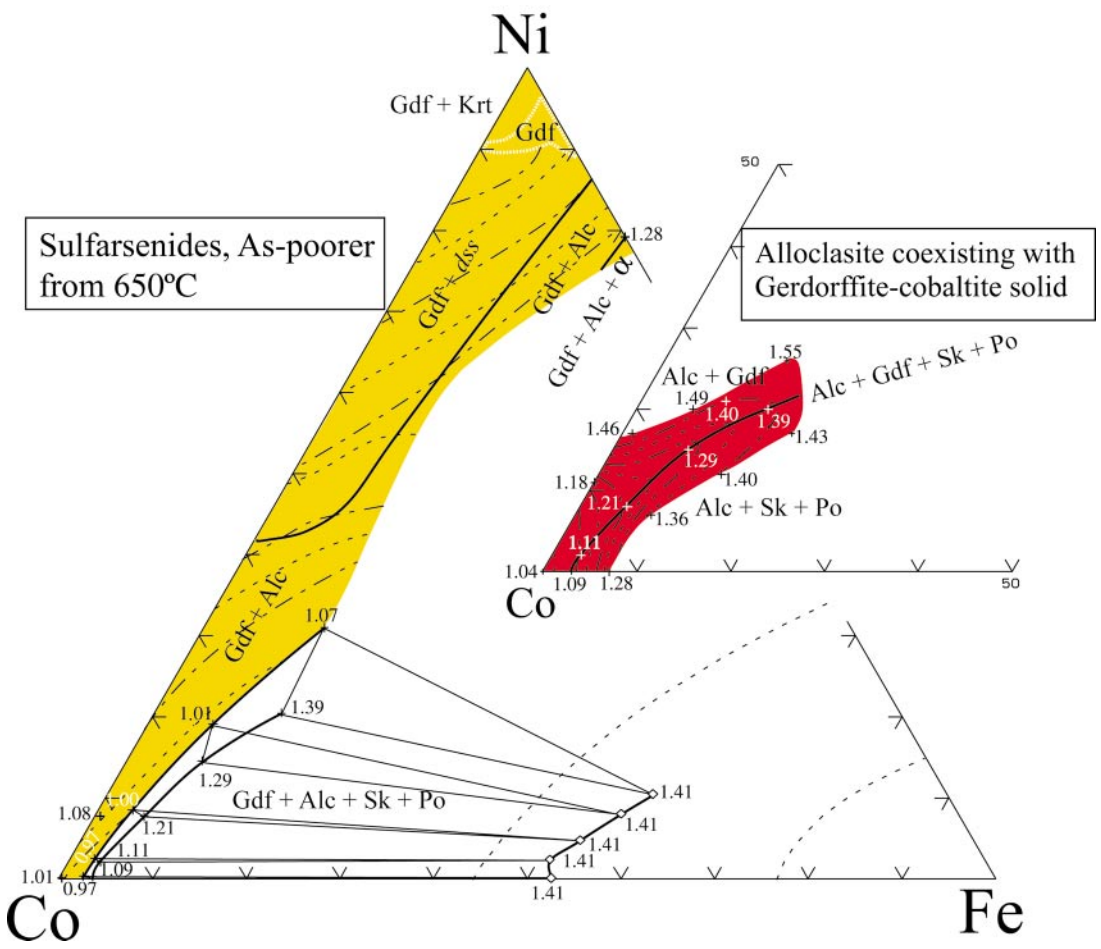

FIG. 12. The compositions of cobaltite–gersdorffite solid-solution and of alloclasite in association with skutterudite and pyrrhotite. This diagram shows a continuation of the cobaltite–gersdorffite solid-solution toward compositions richer in Co and S. The inset figure shows the composition of the coexisting alloclasite. This representation corresponds to the As-poor side of the alloclasite solid-solution volume. The Alc + Gdf + Sk + Po line is shown in both figures. The compositions of cobaltite–gersdorffite and arsenopyrite coexisting at 650°C according to Klemm (1965a) are shown as dotted lines. For notation, see Figure 10.

THE 500°C EXPERIMENTS

The extensive solid-solutions found at 650°C are drastically reduced at 500°C. The diarsenides found are safflorite, löllingite, krutovite and *dss*. The sulfarsenides stable at this temperature are alloclasite, cobaltite, gersdorffite and arsenopyrite. Skutterudite and pyrrhotite still play an important role in the observed equilibria. Jaipurite, nickeline and langisite are found in disequilibrium assemblages. Jaipurite is found enclosed in cobaltite, nickeline in gersdorffite, and langisite in alloclasite or skutterudite. The volume of the (Fe,Co,Ni)$(As,S)_2$ prism investigated is dominated by five-phase assemblages, all including skutterudite and pyrrhotite. The data referred to in the text and Figures 14–17 are listed in Appendix B (deposited) according to the phase assemblage.

DESCRIPTION OF PHASES FORMED AT 500°C

Alloclasite

Alloclasite occurs in equilibrium with safflorite, gersdorffite or skutterudite, and pyrrhotite. It shows a limited incorporation of Fe (<1.4 at.%) and Ni (<2.8 at.%), whereas the As (42.0–52.0 at.%) and S (14.3–24.4 at.%) contents vary widely. Sulfur-rich alloclasite is found together with gersdorffite, cobaltite or

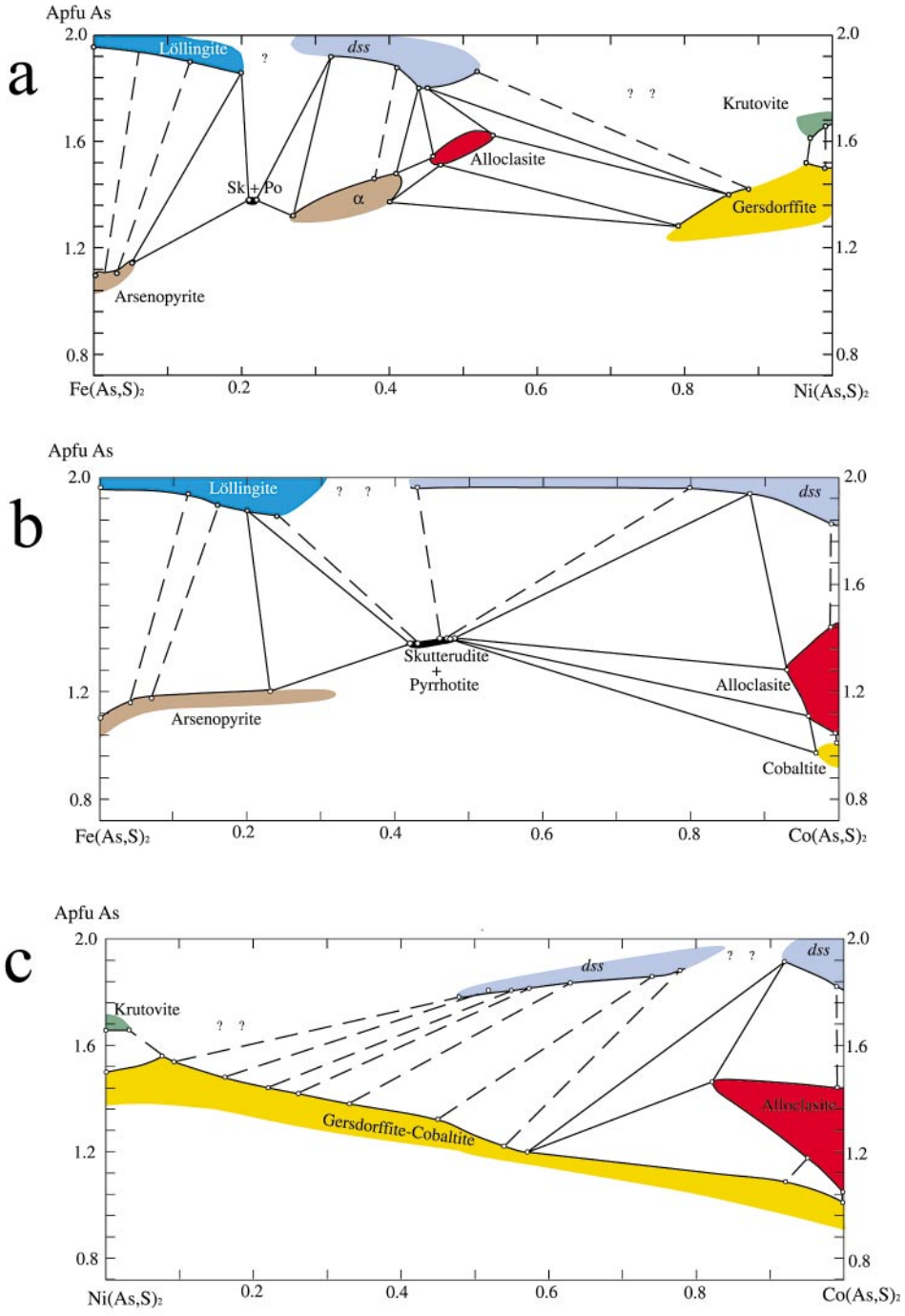

FIG. 13. Binary presentations of the sides of the MeX_2 prism at 650°C, establishing the connection among Figures 10, 11 and 12. The solid lines show the solid-solutions limits for a given phase-association. Compositional variations along the axes are given in *apfu* (MeX_2). The figures show: (a) the Fe–Ni join, (b) the Fe–Co join, and (c) the Ni–Co join.

skutterudite, and pyrrhotite. The Alc + Cbt assemblage was found in only one instance, and both minerals have compositions close to stoichiometry. Toward the As-rich side, the alloclasite solid-solution volume coexists with safflorite, toward the Ni-rich side its limiting compositions coexist with gersdorffite, and toward Fe, it coexists with skutterudite and pyrrhotite (Fig. 14).

Arsenopyrite

Arsenopyrite solid-solution is restricted to compositions close to FeAsS (Fig. 14). It can contain up to 2.2 at.% Ni and 3.4 at.% Co. The As contents range between 34.5 and 36.2 at.%. High Co and Ni contents favor high As contents, though this correlation is weak compared to the uncertainty of the experiment. Compared to the 650°C experiment, the solubility of Co and As is somewhat reduced, whereas that of Ni remains unchanged. Arsenopyrite coexists with löllingite, *dss*, gersdorffite or skutterudite, and pyrrhotite. The arsenopyrite solid-solution field is divided into two areas, a Ni-rich area defined by the coexistence of Apy + *dss* and a Ni-poor area defined by the coexistence of Apy + Lö. In charges having a bulk composition richer in Co and Ni, the arsenopyrite solid-solution coexists with skutterudite and pyrrhotite or gersdorffite.

Gersdorffite

Gersdorffite displays a limited solubility of Fe and Co; it is characterized by high contents of As. At 500°C, it can contain up to 2.8 at.% Fe and 5.4 at.% Co, whereas the As content varies from 44.4 to 49.8 at.%, and content of sulfur correspondingly varies from 16.4 to 22.0 at.%. Relative to 650°C, Fe and As contents are reduced by 1–2 at.%, whereas that of Co is reduced to one sixth of the extent of solid solution. The field of the gersdorffite solid-solution consists of three zones, one coexisting with safflorite, one with krutovite, and one with *dss* (Fig. 14). Along the Co- and Fe-rich limits of the gersdorffite field, alloclasite, skutterudite and pyrrhotite or arsenopyrite are coexisting phases.

Diarsenide solid-solution

The diarsenide solid-solution is restricted to an area close to the Fe-rich portions of the Fe–Ni join, and the contents range from 17.9 to 29.7 at.% Fe, <3.5 at.% Co, from 3.9 to 15.3 at.% Ni, from 61.3 to 65.0 at.%, and from 1.4 to 5.1 at.% S. There is a positive correlation between Fe and As contents. Figure 15 shows these compositions according to the phase assemblages with which they occur. The *dss* field is composed of three areas, a Ni-rich area where *dss* coexists with gersdorffite, a Fe-rich area where *dss* coexists with arsenopyrite, and an intermediate area where it coexists with skutterudite and pyrrhotite. Nickel-rich *dss* coexists with gersdorffite and krutovite, whereas Fe-rich *dss* coexists with arsenopyrite and löllingite. Toward compositions richer in Co, the phase-assemblages are restricted by invariant equilibria with skutterudite and pyrrhotite. The Co-rich limit of *dss* coexisting with skutterudite and pyrrhotite was not determined.

The *dss* phase field is dramatically reduced compared to that determined at 650°C; in particular, the solubility of Co is lowered. In general, *dss* contains sligthly less sulfur and coexists with phases somewhat richer in sulfur than at 650°C. The solid solution stretches toward compositions richer in Fe; this is most likely linked to the shrinkage of the löllingite field at 500°C.

Löllingite, krutovite and safflorite

All these phases display limited solid-solutions, which are confined to compositions close to their stoichiometry (Fig. 15). The Ni diarsenide found in this assemblage is also krutovite, but it is notably richer in As than at 650°C. As discussed in the previous paragraph, equilibria involving *dss* + Lö + Krt were not determined. Parts of all these solid-solution series thus could extend somewhat further than shown in Figure 15. The compositions given in this paragraph all refer to the As-poor side of the solid-solution fields. Phases richer in As than those referred to here are found in local equilibria with skutterudite.

Löllingite contains little Ni (up to 0.8 at.%) and S (0.8–2.2 at.%), but substantial amounts of Co (up to 7.7 at.%). The löllingite solid-solution field is divided into two areas, one that is in equilibrium with arsenopyrite, and one with skutterudite and pyrrhotite. Toward Ni, it is limited by the coexistence with *dss* and arsenopyrite, and toward Co, by skutterudite and pyrrhotite.

The krutovite solid-solution (<1.7 at.% Fe, <1.2% Co, 1.5–4.3% S) consists of one area that coexists with gersdorffite, and another area that coexists with skutterudite and pyrrhotite. The Co-rich members are the richer in sulfur, and the Fe-rich members, the poorer. The Co-rich limit is defined by the Saf + Gdf + Krt and Saf + Krt + Sk + Po equilibria; the Fe-rich boundary is in part limited by the assemblages *dss* + Gdf + Krt and Saf + Lo + Krt + Sk + Po. As opposed to the 650°C experiments, it was possible to identify coexisting krutovite and gersdorffite by PXRD. The unit-cell parameter *a* of (Fe,Co)-free gersdorffite 5.6917(5) Å, and that of the coexisting krutovite, 5.723(1) Å.

The safflorite solid-solution can contain little Ni (<1.0 at.%), and this amount is reduced as Fe is introduced (<7.2 at.%). Up to 6.4 at.% S can substitute for As, and high Co contents favor the incorporation of sulfur. The solid-solution field is subdivided into three areas, respectively coexisting with alloclasite, gersdorffite, or skutterudite + pyrrhotite. The Ni-rich limit coexists with krutovite, and the Co-rich limit coexists with skutterudite and pyrrhotite.

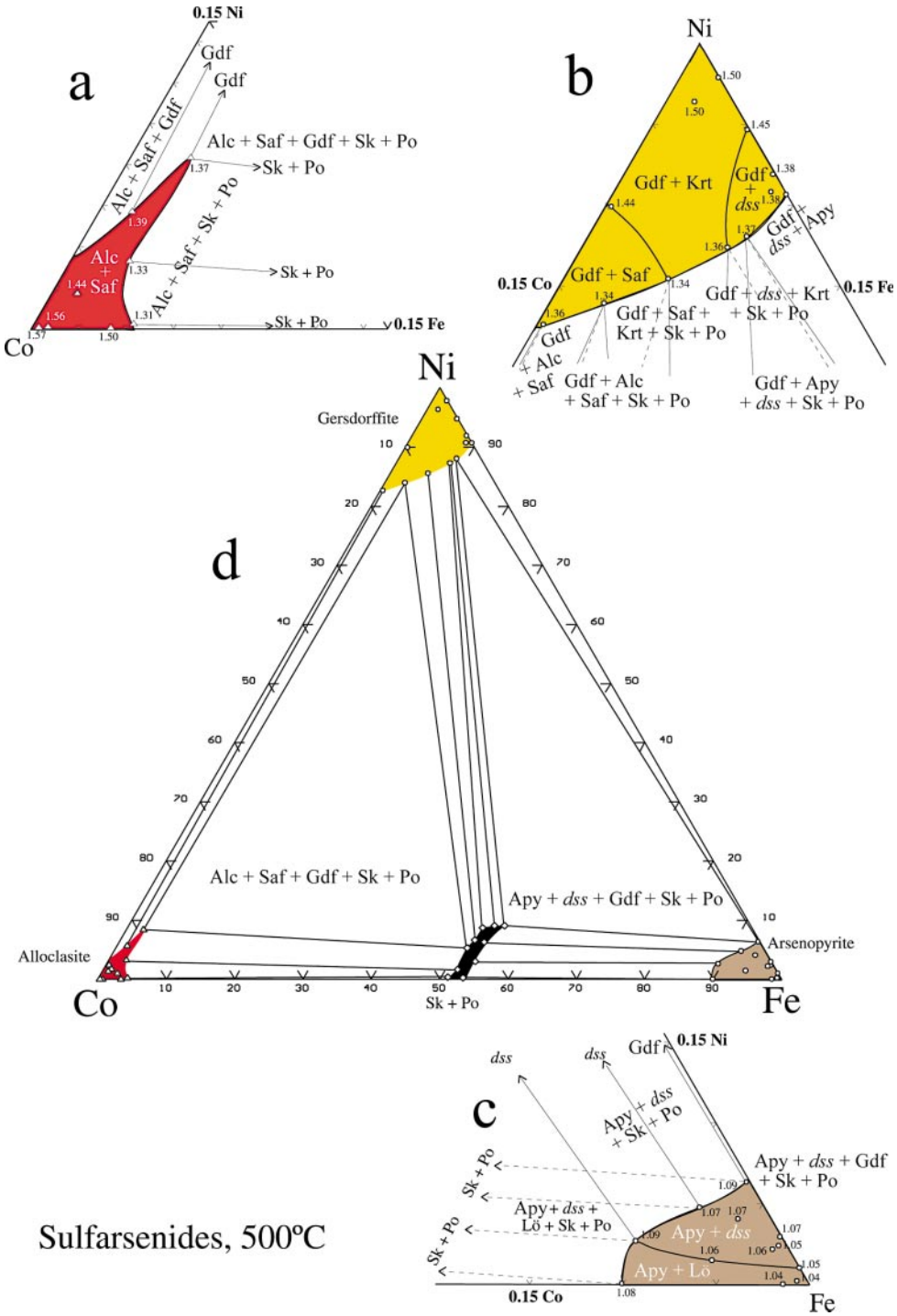

FIG. 14. Contents of Fe, Co, and Ni of sulfarsenides coexisting with diarsenides (Fig. 15) as well as skutterudite and pyrrhotite at 500°C. The solid-solution fields correspond to the As-rich side of the respective solid-solution volumes. The As content and phase assemblages are listed. The intersections of the Sk + Po tielines with the MeX_2 prism are shown in black. Tielines to diarsenides are stippled. Diagrams (a) to (c) show enlarged views of the corners of the triangle in (d).

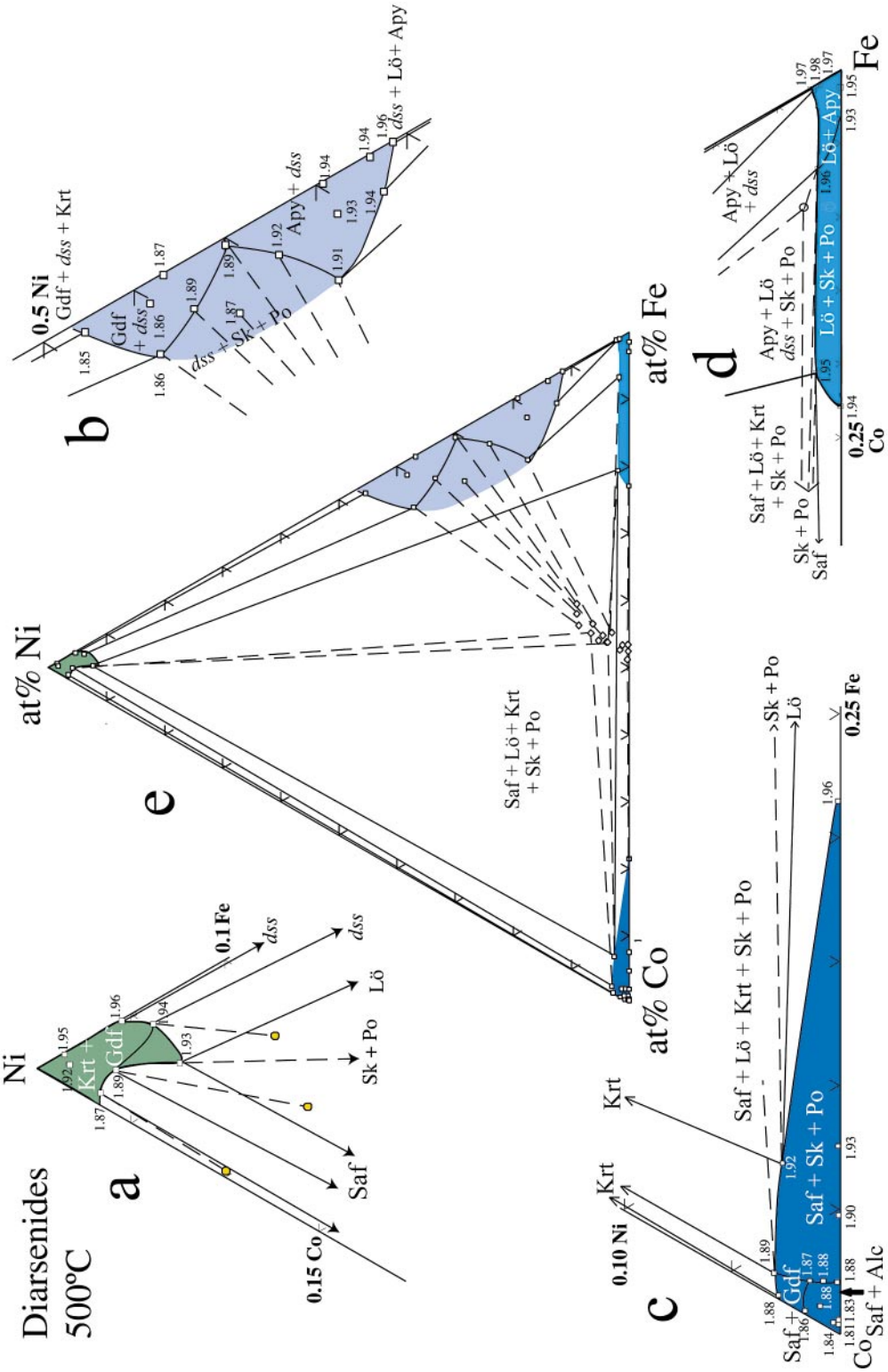

FIG. 15. The compositions of diarsenides in equilibrium with sulfarsenides or skutterudite (or both) and pyrrhotite at 500°C. The solid-solution fields shown correspond to the As-poor sides of the solid-solution volumes. Tielines connecting to sulfarsenides or the Sk + Po intersections are dotted. Diagrams (a) to (d) show enlarged views of the phase fields shown in (e).

Skutterudite

The compositions of skutterudite in equilibrium with pyrrhotite at 500°C are confined to an area close to the Co apex of the Fe–Co–Ni triangle (<2.3 at.% Fe, from 19.0 to 25.3 at.% Co, <4.2 at.% Ni, from 0.5 to 2.7 at.% S, and from 71.5 to 74.4 at.% As). The value Σ*Me* varies from 25.1 to 25.9 at.% , but there is no direct link between this and the phase association, probably because the compositional variation exhibited by skutterudite at 500°C is small compared to that exhibited at 650°C.

The skutterudite solid-solution field is divided into five areas delimited approximately in Figure16. In each of these areas, skutterudite coexists with one of the following phases: alloclasite, *dss*, löllingite, krutovite or safflorite, in addition to pyrrhotite. The Ni-rich limit of the field is associated with gersdorffite, and the Fe-rich limit, with arsenopyrite. Compared to the situation at 650°C, skutterudite formed at 500°C is restricted to compositions much richer in Co.

The skutterudite that does not coexist with pyrrhotite shows a significantly enhanced solubility of Fe and Ni, and Co-free skutterudite (11.0 at.% Fe, 0.0% Co, 15.1% Ni, 0.9% S and 72.9% As) was found overgrown by *dss*.

Pyrrhotite

Pyrrhotite formed at 500°C (45.9–47.8 at.% Fe, <0.5% Co, <1.2% Ni, <0.7% As, 51.6–53.2% S) in equilibrium with skutterudite shows the same compositional pattern as at 650°C; its compositions define two groups in terms Ni contents (Fig. 9). The solubility of Co and Ni is roughly halved. The high-Ni group occurs with gersdorffite, krutovite or *dss*, whereas the low-Ni group occurs with alloclasite. The other phases present in the system coexist with pyrrhotite from both groups. The contents of As are somewhat higher, but vary sporadically. This situation could indicate that the elevated As contents are a result of analytical errors, such as interference from neighboring grains.

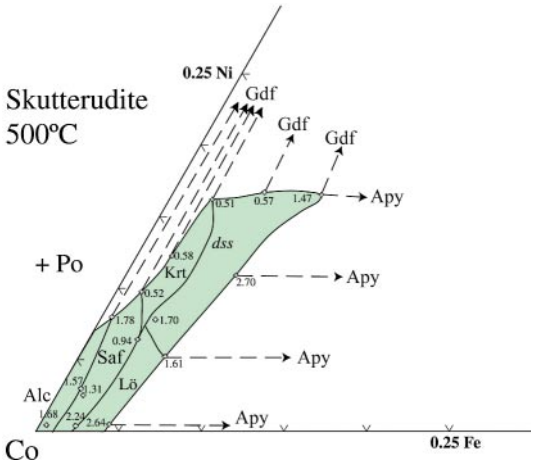

FIG. 16. The skutterudite solid-solution at 500°C. This representation shows the composition of skutterudite coexisting with pyrrhotite in addition to the stated phases. This field corresponds to the As-poor side of a solid-solution volume, but this representation is slightly equivocal, as the *Me*:*X* ratio varies.

The (Fe,Co,Ni)(As,S$_2$) prism at 500°C

The sides of the (Fe,Co,Ni)(As,S)$_2$ prism are shown in Figure 17, as (Fe,Ni)(As,S)$_2$, (Fe,Co)(As,S)$_2$ and (Co,Ni)(As,S)$_2$ diagrams. The sulfarsenide level of the prism is shown in Figure 14, whereas Figure 15 shows the diarsenide level. In order to establish a correspondence between Figures 14 and 15, the intersections of the skutterudite + pyrrhotite tielines with the MeX_2 prism are shown in both the sulfarsenide and the diarsenide diagrams. Chemical characteristics of each phase have been treated in the previous paragraphs.

The chemical volume of the (Fe,Co,Ni)(As,S)$_2$ prism at 500°C is dominated by univariant assemblages, all containing skutterudite and pyrrhotite. The volume of the prism richest in As is filled by the five-phase assemblage Saf + Lo + Krt + (Sk + Po). Below this lie the tetrahedra Saf + Krt + Gdf + (Sk + Po), *dss* + Gdf + Krt + (Sk + Po) and the Apy + *dss* + Lo + (Sk + Po) assemblages. The volume investigated richest in S is filled by the phase volumes Alc + Saf + Gdf + (Sk + Po) and Apy + *dss* + Gdf + (Sk + Po).

DISCUSSION OF THE PHASE ASSEMBLAGES OBSERVED

The experimental results can be compared with naturally occurring phase assemblages as well as with the results of the previous experimental work on relevant systems. The most interesting points are the extent of the solid-solution fields and the nature of the phase assemblages.

In this study, alloclasite is richer in As than it is in nature, although natural alloclasite also has a surplus of As over S, typically in the range 1.01 to 1.22 *apfu* As (Kingston 1971, Vinogradova *et al.* 1975, Scott & Nowacki 1976, Karup-Møller & Makovicky 1979, Hem *et al.* 2001). The extensive solid-solution exhibited by alloclasite at 650°C is not found in natural deposits, and the one found at 500°C is richer in Ni than its naturally occurring counterparts. The reported compositions show resonable agreement with alloclasite synthesized by Maurel & Picot (1974), but these authors found alloclasite to be stable only at temperatures higher than 800°C. In natural deposits, alloclasite occurs with cobaltite, safflorite, skutterudite and arsenopyrite (Petruk *et al.* 1971, Laroussi *et al.* 1992) or gersdorffite (En

Nacri 1995), corresponding well with the assemblages synthesized.

The natural analogue of the $\alpha(Fe_{0.65}Ni_{0.35})As_{1.4}S_{0.6}$ phase formed at 650°C is Ni-rich glaucodot or arsenopyrite. Whether or not this phase is a part of the arsenopyrite solid-solution has yet to be clarified.

The compositions and phase relations of arsenopyrite, cobaltite and gersdorffite are compatible with the naturally occurring phases as described in the literature. Gersdorffite with high As contents is uncommon, but arsenian gersdorffite of composition similar to ours has been reported from several occurrences (Petruk *et al.* 1971, Spiridonova & Chvileva 1995, Ilinca 1998, Fanlo *et al.*, in prep.). The only discrepancy is the limited solubility of Co in arsenopyrite, as it can contain up to 0.6 *apfu* Co in nature (Petruk *et al.* 1971, Grorud 1997). A possible explanation is that arsenopyrite can contain more Co where coexisting with cobaltite, skutterudite and pyrrhotite, a phase volume that was not investigated in this study (Fig. 13).

The solid-solution field exhibited by löllingite and *dss* (safflorite) at 650°C extends toward compositions slightly richer in Ni than the natural analogues (Fig. 18); otherwise there is an overall correspondence between the natural and the synthetic compositions. The gap between *dss* and löllingite, and that between *dss* and $NiAs_2$, are also found in natural phases, and the miscibility gap determined by Roseboom (1963) is not violated. The *dss* – krutovite – gersdorffite assemblage determined at 500°C corresponds well with the mineral compositions reported by Oen *et al.* (1984), both with regard to composition and temperature.

The absence of rammelsbergite and pararammelsbergite in our experiments is caused by the relatively sulfur-rich composition of the charges. Charges containing at least 56–60 at.% As are required for either of these phases to form (Yund 1962). Clarification of phase relations involving pararammelsbergite, rammelsbergite and krutovite requires further experimental studies. Krutovite in our study has compositions that partially overlap with the gersdorffite field as described by Yund (1962).

The skutterudite solid-solution field is restricted compared to the maximum Fe and Ni contents found by Roseboom (1962), but it extends to compositions richer in Fe than the naturally occurring skutterudite (Fig. 18). Skutterudite containing only Fe and Ni formed at temperatures as low as 500°C during our experiments, as opposed to the minimum temperature of 800°C reported by Roseboom (1962). A review of data obtained by Petruk *et al.* (1971), Misra & Fleet (1975), Laroussi (1990), En Nacri (1995), En Nacri *et al.* (1995), Grorud (1997) and Fanlo *et al.* (in prep.) showed that skutterudite is found together with any of the sulfarsenides and diarsenides of Fe, Co and Ni. This is in agreement with the phase assemblages observed in our study. A serious problem is that natural skutterudite only seldom occurs together with pyrrhotite. This may in part be a geochemical feature, as pure Ni – Co – As phases usually form separately from sulfides.

Conclusions

The phase relations in the As-rich portions of the system Fe – Co – Ni – As – S change significantly from 650° to 500°C. At both temperatures, the phase assemblages include the sulfarsenides alloclasite, arsenopyrite, cobaltite and gersdorffite, forming in association with diarsenide solid-solution, löllingite, krutovite and safflorite, in addition to skutterudite and pyrrhotite.

At 650°C, the system is dominated by the large solid-solution fields of alloclasite, cobaltite–gersdorffite, *dss* and skutterudite. Cobalt-free skutterudite and alloclasite were both found. A phase with a composition close to $(Fe_{0.65}Ni_{0.35})As_{1.4}S_{0.6}$ is stable at this temperature, and it has no direct natural analogue. At 500°C, the extensive solid-solutions shrink or break up, and the compositional volume is dominated by five-phase assemblages. Skutterudite coexists with all other phases, but shows a very limited solid-solution field.

The experimental results correspond well to phase assemblages in nature, with the exception of the Fe–Ni–As-rich alloclasite formed at 650°C. Simple geothermometers, such as the arsenopyrite geothermometer, or the solvus diagram of Klemm (1965a), are not applicable to this system owing to the extensive substitutions not dealt with by those geothermometers. The possibility of using the system for geothermometry is limited, as it requires five-phase equilibrium assemblages, or alternatively a very extensive investigation of the relevant partition-coefficients. The extensive compositional zoning and disequilibrium textures typically exhibited by the naturally occurring phases of this system suggest that such an extensive investigation may not be warranted, mainly because the results would be applicable only to a limited number of magmatic deposits.

Acknowledgements

This study is part of a Ph.D. study by S.H. financed by the Faculty of Science at the University of Copenhagen. The electron-microprobe analyses were financed by the Danish Natural Research Council, and the X-ray powder diffraction, by the CNRS–IMN in Nantes, France. The assistance and advice of Berit Wenzell, Helene Almind, John Rose Hansen, Milota Makovicky, Phillipe Leone and last, but not at least, Yves Moëlo are gratefully acknowledged. We also thank Nigel J. Cook, Robert F. Martin and an anonymous reviewer for criticism and suggestions for improvement.

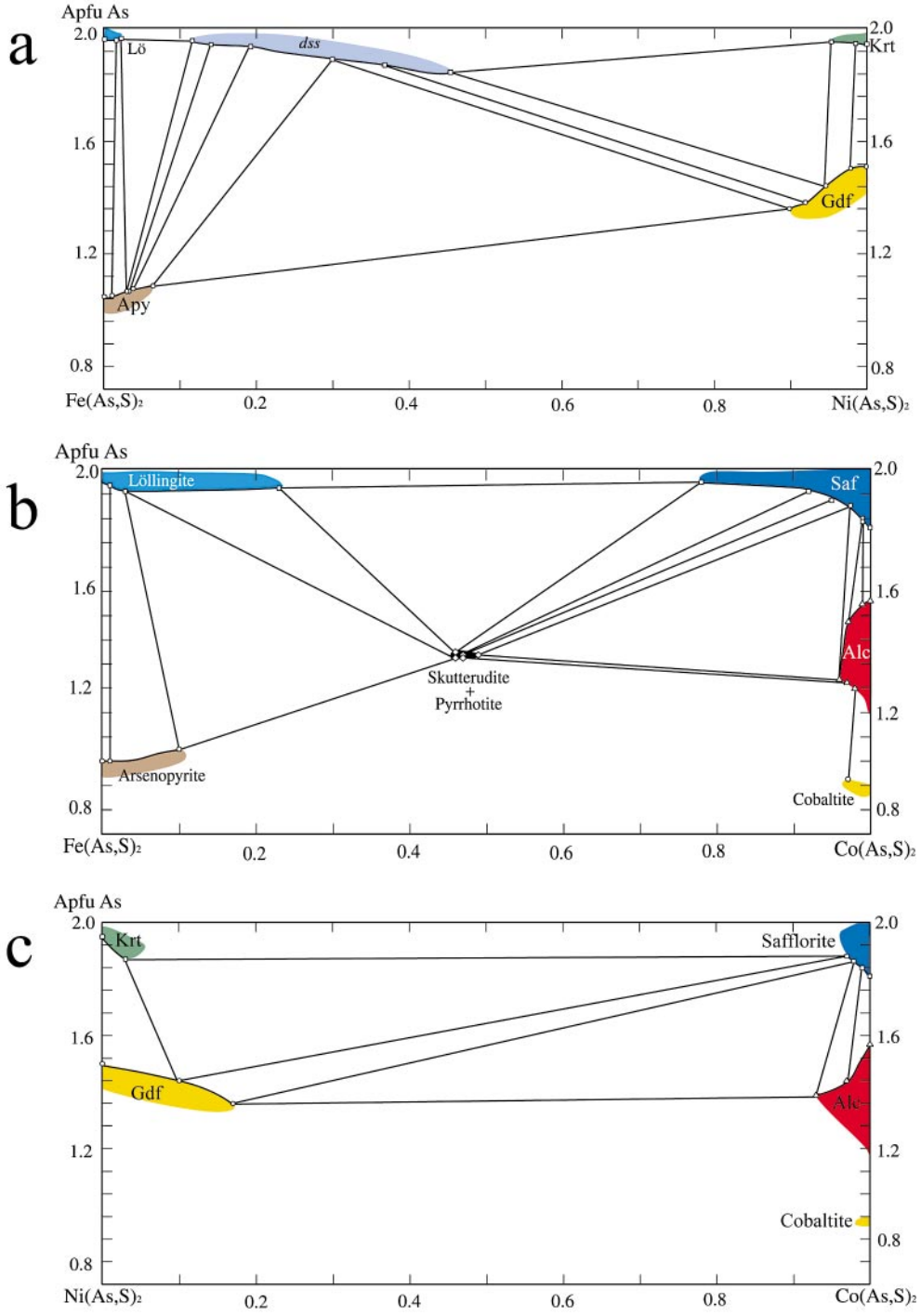

FIG. 17. Binary presentations of the sides of the MeX_2 prism at 500°C. The solid lines show the limits of solid solution for the given phase-assemblages. The axes show the compositional variation in *apfu* (MeX_2) along (a) the Fe–Ni join, (b) the Fe–Co join, and (c) the Ni–Co join.

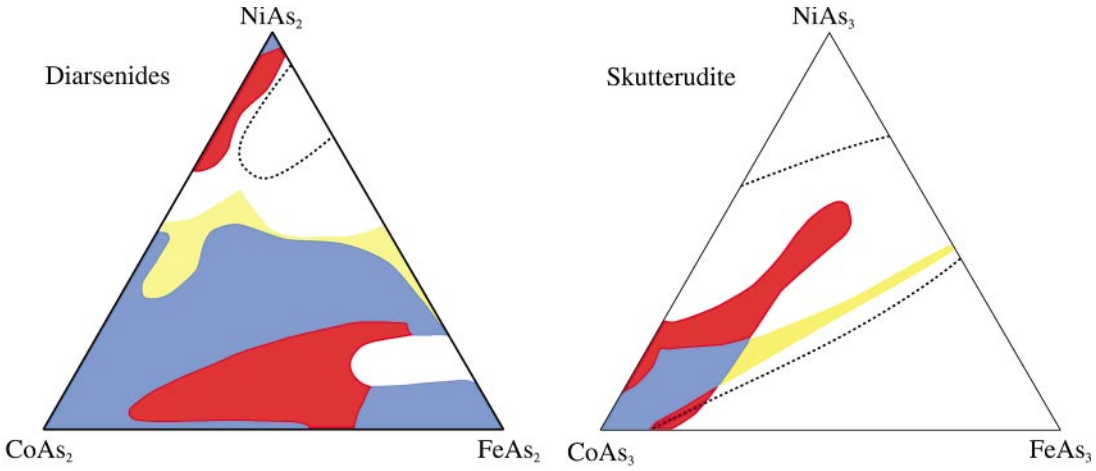

FIG. 18. Compilations of data from literature on diarsenides and triarsenides. On the left: diarsenide compositions; on the right, triarsenide compositions. Compositions from natural occurrences are marked in red, the compositions synthesized in this study, in yellow, and their area of overlap, in blue. The solid-solution fields determined experimentally by Roseboom (1962) are shown by dotted lines. In the diagram showing triarsenides, the solid solution occupies the central area from Co to (Fe,Ni). In the diagram showing diarsenides, the semicircular area marked on the Fe–Ni join represent the only immiscibility gap. Modified after En Nacri (1995), covering data from Radcliffe & Berry (1968), Petruk *et al.* (1971), Laroussi (1990), Gervilla & Rønsbo (1992) and En Nacri (1995).

REFERENCES

BARTON, P.B. (1969): Thermochemical study of the system Fe–As–S. *Geochim.Cosmochim. Acta* **33**, 841-857.

BARKOV, A., THIBAULT, Y., LAAJOKI, K., MELEZHIK, V.A. & NILSSON, L.P. (1999): Zoning and substitutions in Co–Ni–(Fe)–PGE sulfarsenides from the Mount General'skaya layered intrusion, Arctic Russia. *Can. Mineral.* **37**, 127-142.

BAUER, E., GALATANU, A., MICHOR, H., HILCHER, G., ROGL, P., BOULET, P. & NOËL, H. (2000): Physical properties of skutterudites $Yb_XM_4Sb_{12}$, M = Fe, Co, Rh, Ir. *Eur. Phys. J.* **B14**, 483-493.

BAYLISS, P. (1968): The crystal structure of disordered gersdorffite. *Am. Mineral.* **53**, 290-293.

BUERGER, M.J. (1936): The symmetry and crystal structure of the arsenopyrite group. *Z. Kristallogr.* **95**, 83-113.

BURNHAM, C.W. (1993): LCLSQ version 8.5: least squares refinement of crystallographic lattice parameters. Dep. of Earth and Planetary Sciences, Harvard University, Cambridge, Massachusetts 02138, U.S.A.

CLARK, L.A. (1960): The Fe–As–S system: phase relations and application. *Econ. Geol.* **55**, 1345- 1381.

CRAIG, J.R. & SCOTT, S.D. (1974): Sulfide phase equilibria. *Rev. Mineral.* **1**, CS-1 to CS-110.

EN NACRI, A. (1995): *Contribution à l'étude du district à Co, As, (Ni, Au, Ag) de Bou Azzer, Anti-Atlas (Maroc). Données minéralogiques et géochimiques; étude des inclusions fluides*. Thèse de doctorat, Univ. d'Orléans, Orléans, France.

_____, BARBANSON, L. & TOURAY, J.-C. (1995): Mineralized hydrothermal solution cavities in the Co–As Aït Ahmane mine (Bou Azzer, Morroco). *Mineral. Deposita* **30**, 75-77.

FLEET, M.E. (1971): The crystal structure of pyrrhotite Fe_7S_8. *Acta Crystallogr.* **B27**, 1864-1867.

GERVILLA, F. & KOJONEN, K. (2002): The platinum-group minerals in the upper section of the Keivatsanarvi Ni–Cu–PGE deposit, northern Finland. *Can. Mineral.* **40**, 377-394.

_____, LEBLANC, M., TORREZ-RUIZ, J. & FENOLL HACH-ALÍ, P. (1996): Immiscibility between arsenide and sulfide melts: a mechanism for the concentration of noble metals. *Can. Mineral.* **34**, 485-502.

_____ & RØNSBO, J. (1992): New data on (Ni, Fe, Co) diarsenides and sulfarsenides in chromite–niccolite ores from Málaga Province, Spain. *Neues Jahrb. Mineral., Monatsh.*, 193-206.

GIESE, R.F. & KERR, P.F. (1965): The crystal structures of ordered and disordered cobaltite. *Am. Mineral.* **50**, 1002-1014.

GRORUD, H.-F. (1997): Textural and compositional characteristics of cobalt ores from the Skutterud mines of Modum, Norway. *Norsk Geol. Tidsskr.* **77**, 31-38.

HEM, S.R. & MAKOVICKY, E. (2004): The system Fe–Co–Ni–As–S. I. Phase relations in the (Fe,Co,Ni)$As_{0.5}S_{1.5}$ section at 650° and 500°C. *Can. Mineral.* **42**, 43-62.

_____, _____ & GERVILLA, F. (2001): Compositional trends in Fe, Co and Ni sulfarsenides and their crystal-chemical implications: results from the Arroyo de la Cueva deposits, Ronda Peridotite, southern Spain. *Can. Mineral.* **33**, 831-853.

IILINCA, GH. (1998): *Crystal Chemistry of Bismuth Sulphosalts from the Banatitic Province* (*Romania*). Ph.D. thesis, Univ. of Bucharest, Bucharest, Romania (in Romanian).

KARUP-MØLLER, S. & MAKOVICKY, E. (1979): Topotactic replacement of niccolite by rammelsbergite; new data on alloclasite, $Co_{0.56}Ni_{0.45}Fe_{0.01}As_{1.18}S_{0.80}$. *Neues Jahrb. Mineral., Abh.* **136**, 310-325.

KINGSTON, P.W. (1971): On alloclasite, a Co–Fe sulfarsenide. *Can. Mineral.* **10**, 838-846.

KJEKSHUS, A., RAKKE, T. & ANDRESEN, A.F. (1974): Compounds with the marcasite type structure. IX. Structural data for $FeAs_2$, $FeSe_2$, $NiAs_2$, $NiSb_2$, and $CuSb_2$. *Acta Chem. Scand.* **28**, 996-1000.

KLEMM, D.D. (1965a): Synthesen und Analysen in den Dreiecksdiagrammen FeAsS–CoAsS–NiAsS und FeS_2–CoS_2–NiS_2. *Neues Jahrb. Mineral., Abh.* **103**, 205-255.

_____ (1965b): Untersuchungen mit der Elektronmikrosonde über die natürlichen Misch-Kristalbereiche der Skutterudite. *Beitr. Mineral. Petrog.* **11**, 323-333.

KOTNY, A., DE WALL, H., SHARP, T.G. & PÓSFAI, H. (2000): Mineralogy and magnetic behavior of pyrrhotite from a 260°C section at the KTB drilling site, Germany. *Am. Mineral.* **85**, 1416-1427.

KRAUS, W. & NOLZE, G. (1999): *Powder Cell for Windows*, version 2.3. Federal Institute for Material Research and Testing, Rudover Chaussee 5, D-12489 Berlin, Germany.

KRETSCHMAR, U. & SCOTT, S.D. (1976) The phase relations involving arsenopyrite in the Fe–As–S system and their application. *Can. Mineral.* **14**, 364-386.

LAROUSSI, A. (1990): *Etude minéralogique et paragénétique de la minéralisation complexe à Co–Ni–Ag–As des Chalanches* (*Isère*); *comparaison avec le district de Cobalt* (*Ontario*). Thèse de doctorat, Univ. d'Orléans, Orléans, France.

_____, MOËLO, Y., YAMAN, S. & TOURAY, J.-C. (1992): Study of cobaltite and alloclasite in the Esendemir skarn-type ore deposit (Ulukisla–Nigde) by electron microprobe technique. *Turkish J. Earth Sci.* **1**, 57-61.

MADEL, N. & DONAHUE, J. (1971): The refinement of the crystal structure of skutterudite $CoAs_3$. *Acta Crystallogr.* **B27**, 2288-2289.

MAUREL, C. & PICOT, P. (1974): Stabilité de l'alloclasite et de la cobaltite dans les systèmes Co–As–S et Co–Ni–As–S. *Bull. Soc. fr. Minéral. Cristallogr.* **97**, 251-256.

MISRA, K.C. & FLEET, M.E. (1975): Textural and compositional variation in a Ni–Co–As assemblage. *Can. Mineral.* **13**, 8-14.

NICKEL, E.H. (1970): The application of ligand field concepts to understanding of the structural stabilities and solid solution limits of sulphides and related minerals. *Chem. Geol.* **5**, 233-241.

OEN, I.S., DUNN, P.J. & KIEFT, C. (1984): The nickel-arsenide assemblage from Franklin, New Jersey: description and interpretation. *Neues Jahrb. Mineral., Abh.* **150**, 259-272.

PETRUK, W., HARRIS, D.C. & HARRIS, J.M. (1971): Characteristics of the arsenides sulpharsenides, and antimonides. *Can. Mineral.* **11**, 150-186.

PÓSFAI, M., SHARP, T.G. & KOTNY, A. (2000): Pyrrhotite varieties from the 9.1 km deep borehole of the KTB project. *Am. Mineral.* **85**, 1406-1415.

RADCLIFFE, D. & BERRY, L.G. (1968): The safflorite–löllingite solid solution series. *Am. Mineral.* **53**, 1856-1881.

ROSEBOOM, E.H. (1962): Skutterudite (Co,Fe,Ni)As_{3-x}: compositions and cell dimensions. *Am. Mineral.* **47**, 310-327.

_____ (1963): Co–Fe–Ni diarsenides: compositions and cell dimensions. *Am. Mineral.* **48**, 271-299.

SALES, B.C., MANDRUS, D., CHAKOUMAKOS, B.C., KEPPENS, V. & THOMPSON, J.R. (1997): Filled skutterudite antimonides: electron crystals and phonon glasses. *Phys. Rev. B* **56**, 15081-15089.

SCOTT, J.D. & NOWACKI, W. (1976): The crystal structure of alloclasite, CoAsS, and the alloclasite–cobaltite transformation. *Can. Mineral.* **14**, 561-566.

SPIRIDONOVA, E.M. & CHVILEVA, T.N. (1995): On the boundary between gersdorffite NiAsS and krutovite $NiAs_2$. *Dokl. Akad. Nauk* **341**, 785-787 (in Russ.).

VINOGRADOVA, R.A., KRUTOV, G.A. & RUDASHEVSKY, N.S. (1975): A variety of nickel alloclasite. *Dokl. Akad. Nauk SSSR* **222**, 162-164 (in Russ.).

YUND, R.A. (1962): The system Ni–As–S: phase relations and mineralogical significance. *Am. J. Sci.* **260**, 761-782.

Received January 20, 2003, revised manuscript accepted February 28, 2004.